The role of Sp110 in human T cell apoptosis and immunopathology

Inauguraldissertation

zur

Erlangung der Würde eines Doktors der Philosophie

vorgelegt der

Philosophisch-Naturwissenschaftlichen Fakultät

der Universität Basel

von

Fabian Sebastian Baldin

aus Berlin, Deutschland

Basel, 2018

Genehmigt von der Philosophisch-Naturwissenschaftlichen Fakultät

auf Antrag von

Prof. Dr. med. Christoph Hess (Fakultätsverantwortlicher)
Prof. Dr. med. Mike Recher (Dissleiter)
Prof. Dr. med. Nina Khanna (Koreferentin)

Basel, den 26.6.2018

Prof. Dr. Martin Spiess
Dekan

Table of contents

List of tables

1 Introduction

1.1 Primary Immunodeficiency Diseases

Primary immunodeficiency diseases (PID) are genetically determined disorders affecting the functionality of the immune system due to mutations in immune system genes [1]. PID have to be differentiated from secondary immunodeficiencies, that result as a consequence of infections (e.g. human immunodeficiency virus (HIV)), administration of immunosuppressive drugs or hematologic diseases (e.g. lymphoma). The diagnosis of PID may be difficult, since it may clinically manifest through a broad spectrum of different phenotypes including susceptibility to infection but also autoimmune disease, recurrent fever, non-malignant lymphoproliferation (splenomegaly and/or lymphadenopathy), or malignant lymphoma [1].
Currently, more than 350 PID entities have been described [2]. PID that lead to life-threatening infections very early in life due to dysfunctions of both T and B lymphocytes are classified as severe combined immunodeficiencies (SCID) [3]. A very rare, but highly lethal form of SCID is hepatic veno-occlusive disease with immunodeficiency (VODI), which results by a biallelic loss of function mutations in the *SP110* gene, encoding for Sp110 protein [1].

1.2 Veno-Occlusive Disease with Immunodeficiency

VODI was first described in 1976 in three families of Lebanese origin. Six children died in the first year of life due to severe infections and/or hepatic disease. The children suffered from hypogammaglobulinemia, hepatomegaly and various infections, especially pneumocystis pneumonia. Besides veno-occlusive disease of the liver, missing germinal centres in the lymphoid tissues and a low number of mature plasma cells was reported. The disease was reminiscent of a combined immunodeficiency (CID) [4]. In addition, one third of the VODI patients demonstrated neurological disease including microcephaly, hemiparesis or epilepsy [5]. 30 years later, *Roscioli et al.* examined six children (3 - 7 months) from five Lebanese families suffering from VODI. The patients had no germinal centres in examined lymph nodes and liver biopsies showed evidence of veno-occlusion. The patients displayed low concentrations of serum immunoglobulins, low memory B cells and tissue plasma cells. Peripheral B and T cell numbers were typically within normal range for age. Impaired T cell effector function was postulated given the high percentage of severe *Pneumocystis jirovecii* pneumonias [6]. Many patients with non-VODI SCID are successfully treated by bone marrow

transplantation [7]. However, many transplanted VODI patients died due to post-transplant complications [5]. In particular, the pre-transplant conditioning often fatally aggravated the hepatic veno-occlusive disease. Therefore, early substitution with immunoglobulins and pneumocystis prophylaxis with Trimethoprim/Sulfamethoxazole (Bactrim) is the treatment of choice in patients with VODI [6]. However, in 2013 the first VODI patients have been reported to be successfully treated with hematopoietic stem cell transplantation [8]. *Roscioli et al.* mapped the genetic defect in VODI patients to the gene *SP110* encoding for the nuclear body protein Sp110. All patients analysed in that study had homozygous loss-of-protein expression-mutations in this protein [6].

1.3 The PML Nuclear Body Protein Sp110

Nuclear bodies are divided into five different types, categorised by morphology and location [9]. Sp110 is a member of PML nuclear bodies [10]. PML nuclear bodies are thought to be important for cell survival, regulation of gene transcription and apoptosis [11] [12] [13]. *SP110* is located on chromosome 2q37.1 and consists of 2591 base pairs, which corresponds to a 713 amino acid protein subdivided into several functional domains (see **Figure 1b**). Until now, four Sp110 isoforms have been described (see also **Figure 1b**). Isoform A encodes for a Sp110 protein with a truncated bromodomain (NCBI Reference Sequence: NM_004509.3). Isoform B lacks the bromodomain completely (NCBI Reference Sequence: NM_004510.3). The full-length protein of Sp110 is encoded by isoform C (NCBI Reference Sequence: NM_080424.2). Isoform D encodes for a Sp110 protein with a longer N-terminus but a shorter C-terminus compared to the full-length isoform C (NCBI Reference Sequence: NM_001185015.1).

In 1991, autoantibodies against PML- nuclear bodies were reported in sera of patients with primary biliary cirrhosis (PBC) [14,15]. One year later *Szostecki et al.* identified the targeted nuclear protein as Sp100, named according to its molecular weight of 100 kDa [16]. *Bloch et al* identified another PML-nuclear body-autoantigen, named Sp140, that was targeted by sera of PBC patients. Sp140 shares many structural similarities with Sp100 and is also upregulated upon different stimuli such as IFNs [17]. *SP110* was cloned in 2000 by *Bloch et al.* into HEp-2 (HeLa derivative) cells and was described as a new member of the Sp100/Sp140 family [10]. Sp110 contains a Sp100 like domain which can also be found in the other family members [17] (see also **Figure 1b**). This domain has been described to be important for heterodimerization of the different members [18]. The SAND domain, present in all members of

the family is delineated to binding chromatin, functions as a transcriptional regulator and is often associated with the plant homeodomain (PHD) [19 20]. Like the SAND domain, the PHD is present in all SP100/SP140 family members [17]. The PHD activates gene transcription and mediates binding to other nuclear proteins [21]. In addition, a bromodomain is highly conserved in the SP100/SP140 family and is believed to be important for chromatin rearrangement and gene regulation [17 22]. A nuclear localization signal (NLS) located in the middle of the protein is also shared by all family members [10 23]. Since there is the same arrangement of these domains in all SP100/SP140 family members, it is likely that *SP110* acts as a transcriptional activator [10].

SP110 mRNA is maximally expressed in the peripheral blood, in leukocytes and the spleen. Average levels of *SP110* mRNA could be found in the thymus, prostate, testis, ovary, small intestine and the colon. Low levels of *SP110* mRNA are expressed in the heart, brain, placenta, lung, liver, skeletal muscle, kidney and the pancreas [10]. In summary, Sp110 seems to have an expression pattern similar to Sp140 [17]. In addition, as already shown for the other family members, the *SP110* mRNA is increased upon IFN stimulation [10].

Bloch et al. have reported that Sp110 co-localized with Sp100 in PML nuclear bodies and that Sp110 depends on Sp140 to access these bodies [10].

Besides being the causative gene for VODI, Sp110 appears to play a critical role in other diseases. Different groups have reported *SP110* gene polymorphisms to confer susceptibility to or protection from tuberculosis (TB) in different populations such as Indians, Vietnamese or Chinese [24 25 26]. In contrast, many other studies did not find this correlation [27 28]. A murine orthologue of human *SP110* is *Ipr1* which has been described to confer innate immune protection against tuberculosis [29]. Besides the fact that *Ipr1* is located within a homogenous staining region on mouse chromosome 1 and thus highly replicated, homology of murine *Ipr1* and human *SP110* is very limited and most importantly *Ipr1*-deficient mice do not display a VODI-like phenotype [29].

Sp110 is also differentially expressed in autoimmune diseases like systemic lupus (SLE) or malignant lymphoproliferative diseases [30 31 32]. The mechanism of how absent Sp110 leads to the clinical and immunological features of VODI remains unclear.

1.4 Type I interferons (IFN I)

Type I interferons (IFN I), comprising interferon α, interferon β and other related proteins were identified as anti-viral cytokines by transcriptionally activating genes called interferon-

stimulated genes (ISG) which interfere with viral replication [33] [34] [35] [36]. In addition, they have immune-modulatory functions [33] [37]. All IFN I bind to the same receptor, IFNAR, consisting of IFNAR1/IFNAR2 heterodimers [38] [39].

IFNAR dimerization of the receptors enables binding/activation of Janus kinase 1 (JAK1) and tyrosine kinase 2 (TYK2). These kinases subsequently phosphorylate IFNAR resulting in a recruitment of signal transducers and activators of transcription (STAT). In total there are three predominant STAT complexes formed upon the phosphorylation of the receptor. The phosphorylation of the STAT multicomplex promotes the activation of IFN-stimulated genes (ISG) [40]. Until now nearly 1000 ISG have been identified and Sp110 is one of them [10].

PID that are characterized by chronic and inadequate overproduction of ISG are called interferonopathies [1]. These diseases are caused by gain of function mutations in genes controlling ISG formation and associated with neuro-immunologic and autoimmune diseases with a wide clinical spectrum [42]. Polygenic human systemic autoimmune diseases such as systemic lupus erythematosus (SLE) or Sjogren`s syndrome are also linked to elevated ISG [43]. On the other hand, loss of function mutations in IFN-I or its receptor are linked to severe infections [44].

1.5 T cell apoptosis

To guarantee T cell homeostasis, pathogen-specific T cells, following rapid clonal expansion upon infection, have to undergo regulated cell death (apoptosis) after clearance of the pathogen [45]. Furthermore, T cell apoptosis at the peak of T cell reactivity is required to avoid immunopathologic damage of the host [46]. Despite other types of regulated cell death, two main pathways of apoptosis induction have been characterized [47].

Extrinsic apoptosis is induced by ligand binding to death receptors of the tumor necrosis factor (TNF) superfamily [48]. These receptor have in common that all members share a cytoplasmic death domain [49]. The most prominent ligands for these receptors are FasL, TRAIL and TNF-α [50] [51] [52]. The activation of the receptors (CD95, TRAIL receptors and TNFRI) leads, by engaging the death domains to the formation of the multicomplex death-inducing signalling complexes (DISC). These complexes drive the auto-catalytic activation of caspase-8 [53] [54]. Subsequently, activated caspase-8 proteolytically activates the effector caspase-3 and -7 in thymocytes and mature lymphocytes [55].

Intrinsic apoptosis is triggered by different stimuli like toxins, hypoxia or radiation [56]. Central to *intrinsic* apoptosis induction is irreversible mitochondrial outer membrane

permeabilization (MOMP) [57]. MOMP is executed by the proapoptotic BCL-2 family members BAK, BOK and BAX [58] [59]. These proteins are responsible for pore formation in the outer membrane of the mitochondria (OMM) [60] [58]. BAK and BAX are activated by several proapoptotic BH3-only proteins (containing only one BH3 domain), including PUMA, NOXA and BIM whose expression is primarily controlled on a transcriptional level [61] [62] [63] [64] [65]. These proapoptotic BH3-only proteins interact with BAK and BAX, leading to their dimerization and to MOMP [66] [63] [67] [68]. MOMP can be prevented by antiapoptotic proteins of the BCL-2 family such as BCL2, BCL-X_L, MCL1, BCL-W or BFL-1 [58] [69]. These proteins which all express four BH3 domains are located in the OMM and inhibit the oligomerization of BAK and BAX or directly prevent the process of pore forming [70] [58].

Mitochondrial outer membrane permeabilization leads to a release of apoptotic factors out of the mitochondrial intermembrane space [57] [71]. One essential proapoptotic factor is cytochrome C [72]. Released cytochrome C binds the cytosolic apoptotic peptidase activation factor 1 (APAF1) allowing recruitment of pro-caspase-9. Subsequently, a protein multicomplex, the apoptosome is formed and proteolytically activates the initiator caspase-9 [73]. Matured caspase-9 subsequently activates the effector caspase-3 and -7 [74] [75].

Both, the *intrinsic* and *extrinsic* pathway of T cell apoptosis finally leads to typical features of apoptosis like DNA fragmentation, phosphatidylserine exposure and formation of apoptotic bodies [76] [41] [77] [78].

1.6 *Pneumocystis jirovecii* infection

Pneumocystis jirovecii, formerly known as *Pneumocystis carinii,* is a pathogen which belongs to the family of fungi [79] [80]*.* It is transmitted via respiratory droplets and infects the airways of individuals [81]. Pneumocystis infection may cause a severe pneumonia in patients who are immunosuppressed such as patients with HIV, patients treated with systemic steroids or other immunosuppressants, e.g. after organ transplantation [82]. Pneumocystis does not typically lead to severe disease in patients with absent B cells [83], implying that T cell responses rather than antibodies are essential in the anti-pneumocystis immune response. In immunocompetent individuals, pneumocystis induces a self-limited airway infection or is cleared without symptoms [83]. It has been demonstrated that the adaptive T cell response induces immunopathologic lung damage following pneumocystis infection. In a murine model, depletion of T cells was even superior to antibiotic treatment to prevent severe lung

damage [84]. Also in human pneumocystis pneumonia immunosuppression induced by adjunct steroids in addition to antibiotics have resulted in better outcomes [85].
In VODI patients, early immunoglobulin supplementation by intravenous immunoglobulins (IVIG) and *Pneumocystis jirovecii* prophylaxis by Trimethoprim/Sulfamethoxazole (Bactrim) improves the course of disease [6 86].

In this thesis we addressed the question how absent Sp110 alters T cell function. Specifically, our aim was to analyze whether absent Sp110 might alter activation induced T cell apoptosis which might impact on T cell driven immunopathology following pneumocystis infection.

2 Methods

2.1 Isolation of PBMC/generation of T cell blasts

For generation of primary T cell blasts from healthy individuals, EDTA blood tubes or buffy coats were received from the blood donation centre Basel following informed consent. EDTA blood from VODI patients was obtained following informed consent according to protocol 04-09-113R approved by the Boston Children's Hospital Institutional Review Board. ETDA-blood was mixed 1 to 1 with phosphate buffered saline (PBS) (Sigma-Aldrich). The diluted EDTA blood was then layered over a gradient of lymphoprep (Axis-Shield) in a 50 ml Falcon tube. Subsequently the tube was centrifuged for 20 min at 1800 rpm using the settings *acceleration 4* and *brake 1*. By centrifugation of the blood through the lymphoprep gradient, different cell fractions were separated. From top to bottom the first layer contained the plasma, followed by a layer which contained the peripheral blood mononuclear cells (PBMC) and platelets. The next layer consisted of the lymphoprep reagent. Directly on top of the erythrocytes there was a small whitish layer containing the granulocytes. Erythrocytes were located at the bottom of the tube following centrifugation. PBMC were isolated by careful pipetting and washed with 50 ml PBS. Afterwards the solution was centrifuged for 5 minutes at 1800 rpm. If the cell pellet contained too many erythrocytes a lysis step using an erythrocyte lysis buffer (Qiagen) was performed. Therefore the pellet was re-suspended in 1 ml of lysis buffer for 5 minutes at room temperature (RT). Afterwards cells were washed with 50 ml PBS and centrifuged. In the next step the cell pellet was resuspended in RPMI-medium and the concentration of the cells was determined by an EVE Automatic cell counter (NanoEnTek). Subsequently, 3 x 10^6 cells/ml PBMC were seeded on a 96-well U-bottom plate. To generate T cell blasts PBMC were stimulated with 5 µg/ml PHA (Sigma-Aldrich) and IL-2 (300 IU/ml, Novartis). Every 4-7 days, T cell blasts were expanded 1:1 in new medium containing fresh IL-2. While PBMC derived T cells normally had more $CD4^+$ T cells compared to $CD8^+$ T cells, the $CD4^+/CD8^+$ T cell ratio was typically < 1 in expanded T cell blasts (see **Figure 3**).

2.2 Jurkat T cells

Jurkat T cells were first isolated in 1977 form a patient with T cell leukemia [87]. In this thesis all Jurkat T cell based experiments were performed using the Jurkat clone E6.1 as parental Jurkat T cell line ($SP110^{wt}$).

2.3 Cell culture

Jurkat T cells and primary PBMC-derived T cell blasts were cultured in RPMI-medium (Sigma-Aldrich) containing 100 U/ml Penicillin-Streptomycin (Gibco), 5 ml of 100 x MEM Non-Essential Amino Acids Solution (Gibco) and 5 ml of 100 x GlutaMAX (Gibco) per 500 ml RPMI-medium. Full medium contained 10% fetal calf serum (FCS, Gibco). T cells were cultured using the following settings: 5% CO_2, 18% O_2 and 37°C. Before every experiment, cell viability and cell numbers were controlled using an EVE Automatic cell counter (NanoEnTek).

2.4 Reagents for cell stimulation

Primary PBMC derived T cell blasts or Jurkat T cells were stimulated with different reagents to induce cell activation and related apoptosis. T cells were transferred to a 96-well U-bottom plate at 3 x 10^6 cells/ml and stimulated with reagents/inhibitors as listed in Table 1. Unless otherwise stated, primary T cell blasts or Jurkat T cells were stimulated for four hours in the incubator prior to analysis of T cell apoptosis. Specific inhibitors of signalling pathways were used at the concentrations listed in **Table 1** and were added 30 minutes prior to cellular stimulation.

Table 1 Reagents and inhibitors used for stimulation of primary T cells and Jurkat T cells

Reagents	**Final conc.**	**Company**
PMA	5 ng/ml	Sigma-Aldrich
Anti-human CD95/Fas (EOS9.1)	5 µg/ml	Biolegend
Interferon α-2a	3000 IE/ml	Roche
Inhibitors		

C Jun N terminal kinase inhibitor (SP600125)	100 µM	Sigma-Aldrich
panSTAT inhibitor (SH-4-54)	100 nM	Sigma-Aldrich
JAK1/2 inhibitor Ruxolitinib	10 µM	Sigma-Aldrich

2.5 Ultraviolet-light irradiation

To induce apoptosis by UV-light, primary T cell blasts or Jurkat T cells were irradiated with UV-C light (254 nm) at doses ranging from 50 J/m^2 – 200 J/m^2. The irradiation was done in a Stratalinker UV Crosslinker 1800 UV-chamber (Stratagene).

2.6 Flow cytometric analysis for intracellular/nuclear proteins or protein phosphorylation

To determine intracellular protein expression or intracellular protein phosphorylation, primary T cell blasts or Jurkat T cells were fixed at room temperature (RT) for 20 min with Fix/Perm buffer (BD Biosciences). After fixation and washing in 2% FCS/PBS, cells were permeabilized with Perm III Buffer (BD Biosciences) at 4°C for 30 min. The primary (unlabeled) antibody was diluted 1:100 in 2% FCS/PBS and added to the cells for 45 min at RT (**Table 2**). Non-specific isotype control or normal rabbit IgG served as non-specific staining controls. Following washing in 2% FCS/PBS, the cells were incubated for 30 min at RT with Alexa Fluor 488/647 – conjugated secondary antibodies directed against the primary antibody (e.g. anti rabbit IgG, Jackson ImmunoResearch) diluted 1:100 in 2% FCS/PBS for 45 minutes. Protein expression or protein phosphorylation was determined on a CytoFLEX (Beckman Coulter) or BD Accuri C6 (BD Biosciences) and the analysis was performed using FlowJo software (FlowJo LLC).

Table 2 Primary and secondary antibodies used to detect intracellular proteins or protein phosphorylation

Primary antibodies	Final conc. (µg/ml)	Company
Sp110 rabbit polyclonal IgG	1.6	Proteintech
p-c-Jun (Ser73) rabbit monoclonal IgG	0.35	Cell Signaling

pSTAT1 (Tyr701) (58D6) rabbit monoclonal IgG	0.45	Cell Signaling
pSTAT3 (Tyr705) (D3A7) rabbit monoclonal IgG	0.45	Cell Signaling
Rabbit control polyclonal IgG	Adjusted	Proteintech
Rabbit isotype control monoclonal IgG (DA1E)	Adjusted	Cell Signaling
Secondary antibody		
Alexa Fluor 488 Fab_2 Fragment goat anti-rabbit IgG	0.75	Jackson ImmunoResearch
Alexa Fluor 647 Fab_2 Fragment goat anti-rabbit IgG	0.75	Jackson ImmunoResearch

2.7 Flow cytometry assay to detect cell-surface proteins

To assess the expression of surface proteins by flow cytometry, primary T cell blasts or Jurkat T cells were washed in 2% FCS/PBS and stained with 1:100 diluted fluorochrome-labeled antibodies for 30 min at room temperature (**Table 3**). To confirm the specificity of the staining cellular aliquots were stained with a respective isotype control. Subsequently, cells were washed in 2% FCS/PBS. The protein expression was measured afterwards on a CytoFLEX (Beckman Coulter) or a BD Accuri C6 (BD Biosciences). Analysis of the data was performed using FlowJo software (FlowJo LLC).

Table 3 Primary antibodies for cell surface staining

Antigen (clone)	Fluorochrome	Conc. (µg/ml)	Company
AnnexinV	FITC, APC	0.5	Biolegend
CD3 (UCHT1)	PE, PE/Cy7, APC	0.5	Biolegend
CD4 (SK3)	PE/Cy7	0.5	Biolegend
CD8 (SK1)	PE, PE/Cy7	0.5	Biolegend
CD27 (O323)	FITC, APC	0.4	Biolegend
CD45RO (UCHL1)	PE	0.1	Biolegend
Isotype Ctrl	FITC, PE, PE/Cy7, APC	Adjusted	Biolegend

2.8 Detection of apoptosis by flow cytometry

Primary T cell blasts or Jurkat T cells, either left unstimulated or treated with the indicated inducers of apoptosis (see **Table 1**), were cultured for four hours. Afterwards, cells were washed twice with AnnexinV Binding Buffer (Biolegend) and stained with 1 µg/ml FITC/APC-labeled AnnexinV, 1:100 diluted in AnnexinV Binding Buffer, for 30 min at RT to detect apoptosis-associated phosphatidylserine exposed at the cell surface. Subsequently, the cells were washed again with AnnexinV Binding Buffer. Apoptotic T cells displaying binding of fluorochrome labelled AnnexinV were enumerated using a CytoFLEX flow cytometer (Beckman Coulter) and the data were analyzed with FlowJo software (FlowJo LLC).

2.9 Flow cytometric analysis of caspase-9 activity

To assess caspase-9 activity by flow-cytometry, 5 x 10^5 cells/sample primary T cell blasts were stimulated with different stimuli (see **Table 1**). Four hours later, cells were incubated for additional 30 minutes in medium containing fluorescently labelled caspase-9 inhibitor FAM-FLICA (ImmunoChemistry Technologies). The staining procedure was performed according to the manufacturer`s protocol. Caspase-9 activity was measured on a BD Accuri C6 (BD Biosciences) and subsequently analyzed with FlowJo software (FlowJo LLC).

2.10 siRNA knockdown of specific genes in Jurkat T cells and primary T cell blasts

Transient transfection with siRNA was performed with the AMAXA Nucleofection Kit T cell (Lonza Group Ltd.) for transfecting primary T cell blasts or AMAXA Nucleofection Kit V (Lonza Group Ltd.) for Jurkat T cells. 5 x 10^6 cells/sample primary T cell blasts or 2 x 10^6 cells/sample Jurkat T cells were transfected by electroporation according to the manufacturer's protocol. The following *SP110* specific and non-specific siRNAs were used:
500 nM Flexi Tube siRNA Hs SP110 1/4/5/6/9/10 and 11 (Qiagen)
500 nM AllStars Neg. Control siRNA (Qiagen)
After electroporation the cells were transferred into pre-warmed RPMI medium and rested for 24 hours at 37°C. Gene knockdown efficacy was tested afterwards by real-time PCR or by measurement of Sp110 protein expression by flow cytometry. Prior to apoptosis induction

using the stimuli listed in **Table 1**, enrichment for live cells using a magnetic bead-based dead cell removal Kit (Miltenyi Biotec) and LS Columns (Miltenyi Biotec) was executed. The procedure was done according to the manufacturer`s protocol.

2.11 Generation of *SP110* knockout Jurkat T cells

To knockout *SP110* in Jurkat T cells, 2 x 10^6 cells/sample were transfected by electroporation with a predesigned *SP110* CRISPR/Cas9 Ko plasmid mix (Santa Cruz Biotechnology Inc.) containing three different *SP110* specific sgRNAs, the Cas9 endonuclease and P2A-EGFP. 24 hours later, cells were sorted for GFP expression on an Aria III cytometer (BD Biosciences) and single cells were plated on a 96-well U-bottom plate. After 2 - 3 weeks of single cell clone-expansion, cDNA was generated from individual clones and a specific PCR was performed, amplifying a 461 bp *SP110* fragment, covering the region that was targeted by the guide RNA. The amplified PCR product was run on a 1.5 % agarose gel, cut, isolated and sequenced by Sanger sequencing to detect insertions/deletions (**Table 4**). To confirm that *SP110* knockout Jurkat T cell clones indeed lacked Sp110 protein, a Sp110 specific flow cytometry staining was performed (**Figure 2**). The detailed molecular analysis of the $SP110^{ko}$ Jurkat T cell clone has been published [88].

Table 4 CRISPR/Cas9 derived T cell Jurkat clones

Clone	Modification	Sp110 protein expression
$SP110^{ko}$	Insertion of 8 bp	Knockout
$SP110^{wt}$	None	Basic expression

2.12 Lentiviral transduction

For Sp110 overexpression in Jurkat T cells, 5 x 10^4 cells/sample $SP110^{ko}$ Jurkat T cells were plated on a 12- well plate and incubated with different volumes of the Sp110 overexpressing lentivirus provided by Donald Bloch, Massachusetts General Hospital, Boston, USA. Two different lentiviruses contained transgenes either encoding for full length Sp110 (isoform C) or red fluorescence protein (RFP) as a transduction control. In addition both viruses encoded for a green fluorescent protein (GFP) (**Table 5**). For transduction, the lentivirus-containing supernatant was thawed on ice and a transduction-solution was prepared. 957 µl RPMI-

medium (Sigma-Aldrich) was mixed with 8 µl Polybrene (1mg/ml, Sigma-Aldrich). Subsequently 35 µl of the lentiviral supernatant were added to the solution. Subsequently, $SP110^{ko}$ Jurkat T cells were incubated with the mix. Cells were then centrifuged for 90 min at 800g and incubated over night at 37°C. On the following morning, the lentiviral supernatant was removed and fresh medium was added. One week after transduction, cells with high GFP expression were sorted on an Aria III cytometer (BD Biosciences) and single cells were plated on a 96-well U-bottom plate. Sp110 expression was detected on individual clones by flow cytometry and $SP110^{hi}$ expressing clones were propagated. Jurkat T cell clones with high red fluorescence ($SP110^{ko}$) served as a transduction control.

Table 5 Lentiviral transduced Jurkat T cell clones

Clone	Transduced constructs	Sp110 protein expression
$SP110^{ko}$	*RFP + GFP*	Knockout
$SP110^{hi}$	*SP110 + GFP*	Overexpression

2.13 Protein quantification by western blot

To detect protein expression by western blot, 2 x 10^6 cells/sample Jurkat T cells were washed in PBS and mixed with protein lysis buffer. This buffer contains 50 mM HEPES pH 7.9, 250 mM NaCl, 20 mM glycerophosphate, 5 mM Na_2-4-nitrophenylphosphate, 1 mM EDTA-Na_2, 1 mM Na-orthovanadate, 0.5% (v/v) Nonidet P-40, 10% (v/v) glycerol, 5 mM DTT and protease inhibitors (Sigma-Aldrich and Roche). Subsequently, the suspension was shaken for 20 min at 4°C. Afterwards, the solution was sonicated using a W-375 sonicator/ cell disruptor (Heat Systems-Ultrasonics Inc.). To remove the non-digestible part of the cells the solution was centrifuged at 12.000 rpm for 15 min at 4°C. The protein concentration of the cell lysate was determined by a Pierce BCA Protein Assay Kit (Thermo Fisher Scientific). The procedure was done according to the manufacturer`s protocol.

For western blotting, 20 µg protein/sample were diluted in 2 x Laemmli buffer (Bio-Rad Laboratories) and loaded on a 4-15% Mini-PROTEAN TGX 1-D polyacrylamide gel (Bio-Rad Laboratories). The settings for the separation were 100 V/ 0.2 A for 1.5 hours. Following electrophoresis, gels were transferred onto a 0.2 µm nitrocellulose Trans-Blot Turbo membrane (Bio-Rad Laboratories). To prevent unspecific binding, the blot was washed with TBS/T with 5% BSA (Sigma-Aldrich) for one hour at RT. The membrane was then incubated with the indicated dilutions of primary antibody diluted in TBS/T rotating over night at 4°C (**Table 6**). On the next morning, the blot was incubated with the indicated dilutions of the

fluorochrome-coupled secondary antibodies diluted in TBS/T shaking for one hour at 37°C and subsequently blot-fluorescence was visualized using the ODYSSEY CLx (LI-COR).

Table 6 Primary and secondary antibodies for Western blotting

Primary antibody	**Final conc. (ng/ml)**	**Company**
Caspase-9 rabbit IgG monoclonal	42	Cell Signaling
Secondary antibody	**Final conc. (ng/ml)**	**Company**
IRDye 800 CW goat anti-rabbit IgG (H+L)	100	Licor

2.14 DNA isolation

For DNA isolation, 5 x 10^6 cells/sample primary T cell blasts or Jurkat T cells were pelleted by centrifugation. DNA isolation from cell pellets was done using a QIAmp DNA Blood Mini Kit (Qiagen). The isolation was done in accordance to the manufacturer`s protocol. Following purification, the DNA concentration was determined using a NanoDrop (Thermo Fisher Scientific).

2.15 Endpoint PCR

The amplification of the template DNA was performed using the GoTaq G2 DNA Polymerase (Promega) in the presence of *SP110* isoform specific primer pairs (**Table 7**). The primer concentration was set to 0.5 µM.

Table 7 Primer used for endpoint PCR

Gene	**Sequence forward/reverse**	**Company**
SP110 isoform A	TCTAAGACCCTGGAGAGGCA ATGGTTGCGAAACATCAGGC	Microsynth
SP110 isoform B	TTTGCTCTGTCCTCCAAGAA TCCCCATCCCAAATTAACTATGC	Microsynth
SP110 isoform C	TGAAGGCCTACTGTCATCCA ACCAGGTCCAACCACATTGC	Microsynth

SP110 isoform D	TTGCCTAACTAGCTGACGTG ATGGCTCTTGTCATGGTGAACA	Microsynth

The PCR was performed on a TProfessional TRIO PCR Thermocycler (Core Life Sciences) and according to the manufacturer`s protocol. The specific program for the reactions was:

Table 8 Settings for endpoint PCR

Temperature (°C)	Time (sec)	Cycles
95	120	1
95	20	38
62	20	
72	45	
72	300	1

PCR products were separated and visualized on a 1.5 % agarose gel (Sigma-Aldrich) using a Molecular Imager Gel Doc XR+ (Bio-Rad).

2.16 RNA isolation and cDNA synthesis

5 x 10^6 primary T cell blasts or Jurkat T cells were lysed in Trizol (Thermo Fisher Scientific) and subsequently mixed with chloroform (Sigma-Aldrich). The isolation was performed using the QIAamp RNA Blood Mini Kit (Qiagen) according to the manufacturer`s protocol. The concentration of the RNA was determined by a NanoDrop (Thermo Fisher Scientific). RNA samples were treated with DNase I – Amplification Grade Kit (Sigma-Aldrich) to eliminate DNA. For cDNA synthesis, 100 ng/µl - 1 µg/µl RNA was mixed with random primer (Promega) and placed in a TProfessional TRIO PCR Thermocycler (Core Life Sciences) at 70°C for 5 min for primer annealing. The reverse transcription polymerase chain reaction was performed according to the companies protocol “GoScript Reverse Transcription System”.

2.17 Analysis of mRNA expression by real-time PCR

Gene-specific mRNA expression was quantified by real-time PCR. Most gene-specific primer (listed in **Table 9**) were designed using the NCBI Gene Databank/Primer-BLAST and synthesized by the company Microsynth. *SP110* and *IFNγ* mRNA specific real-time PCR

primer were purchased (Qiagen). Real-time PCR was performed with the GoTaq qPCR Master Mix (Promega) and primer concentrations set to 0.5 µM.

Table 9 Primer used for real-time PCR analysis

Gene	Sequence Forward/reverse	Company
SP110	n/a	Qiagen
18s	GCTTAATTTGACTCAACACGGGA AGCTATCAATCTGTCAATCCTGCT	Microsynth
IPO8	TCCTTGGCCTAAAGCAGGTC ACTGCATTGCTTGAGCAGTTA	Microsynth
Actin	CAACCGCGAGAAGATGACCC AGAGGCGTACAGGGATAGCA	Microsynth
GAPDH	GGTCACCAGGGCTGCTTTTA TTCCCGTTCTCAGCCTTGAC	Microsynth
PUMA	GAAATTTGGCATGGGGTCTGC GGGGAGCTGCCCTCCT	Microsynth
BIM	CTCTCGGACTGAGAAACGCA CGCAGGCTGCAATTGTCTAC	Microsynth
NOXA	AGTTGGAGGCTGAGGTTCCC TTGAGTAGCACACTCGACTTC	Microsynth
IFNγ	n/a	Qiagen
TNFα	GCCTCTTCTCCTTCCTGATCG AGAGGGCTGATTAGAGAGAGG	Microsynth

The PCR was done in a TProfessional TRIO PCR Thermocycler (Core Life Sciences) with the following settings:

Table 10 Settings for real-time PCR

Temperature (°C)	Time (sec)	Cycles
50	120	1
95	600	1
95 60	15 60	40

Unless otherwise stated, cDNA expression of the gene of interest was always normalized to the house keeping genes *18s* and/or *IPO8*. The results were calculated using the method designed by Michael W. Pfaffl using the cycle numbers of specific gene detection [89].

3 Results

3.1 Application of molecular tools to measure T cell intrinsic Sp110 protein quantity and to functionally study T cells with Sp110 over- *vs.* non-expression

The diagnosis of Sp110 deficiency has been challenging partly due to the fact that quantification of Sp110 protein has only been possible using time-consuming techniques (e.g. immunofluorescence microscopy of EBV immortalized B cell lines) [86]. In addition, our own experiments demonstrated that many commercially available Sp110-specific antibodies, due to non-specific binding, cannot be used to distinguish cells expressing *vs.* non-expressing Sp110 protein (data not shown).

In a recently published report by *Marquardsen/Baldin et al. in the Journal of Clinical Immunology,* we have established an easy to perform, rapid flow cytometric test to quantify Sp110 protein in human T lymphocytes [88]. This flow cytometric test, using a commercially available polyclonal IgG rabbit anti-serum against Sp110, has been validated for its ability to diagnose Sp110 deficiency in five patients suffering from VODI. A reprint of this manuscript is attached to the PhD Thesis.

The clinical and molecular characteristics of the patients with Sp110 deficiency (VODI) that were enrolled for the subsequent studies discussed in this PhD thesis are summarized in **Table 11**.

Table 8 Clinical and molecular characteristics of patients with Sp110 deficiency

Pat. nr.	*SP110* mutation	Gender	Age at diagnosis	Current age	Clinical complications	Treat-ment
1	642delC/ 642delC	Female	3 months	8 years	Pneumocystis pneumonia, liver fibrosis	IVIG, Bactrim
2	642delC/ 642delC	Female	4 months	5 years	Recurrent pulmonary and intestinal infections, subacute pancreatitis	IVIG, Bactrim
3	78_79delinsAT/ 78_79delinsAT	Female	3 years	11 years	Pneumocystis pneumonia, veno-occlusive disease of the liver	IVIG, Bactrim

4	T80C/T80C	Male	9 months	10 years	Liver fibrosis, recurrent sinusitis, thrombocytopenia	IVIG, Bactrim

IVIG: intravenous immunoglobulin substitution

Figure 1a representatively depicts Sp110 flow cytometric analysis of peripheral blood derived T cells of a patient with VODI (patient nr. 3), two clinically healthy siblings carrying a disease-causing *SP110* mutation heterozygously and a non-related control. The results indicate that the flow-based assay to quantify Sp110 expression in T cells is not only able to identify the patient, but also the clinically healthy carriers of disease-causing *SP110* mutations (intermediate Sp110 expression).

Sp110 protein, encoded by 19 exons, contains different functional domains consisting of domains accountable for interactions with other proteins (SP110 like domain) or with DNA (SAND domain, PHD domain and bromodomain) [10]. Besides the full-length *SP110* isoform (isoform C), other isoforms have been described, encoding for truncated Sp110 proteins lacking part of the bromodomain (isoform A), completely lacking the bromodomain (isoform B) or having a different C-terminus (isoform D) (NCBI gene 2018) (**Figure 1b,** adapted from [90]). Endpoint PCR specific for the four *SP110* isoforms were performed on T cell blast derived cDNA from a healthy individual or VODI patient nr.1 demonstrating that all *SP110* isoforms are expressed in primary human T cell blasts. Since the homozygous 642delC *SP110* mutation in VODI patient nr.1 does not lead to complete loss of *SP110* mRNA expression, all four mRNA isoforms were also detectable in the VODI patient-derived T cell blasts (**Figure 1c**).

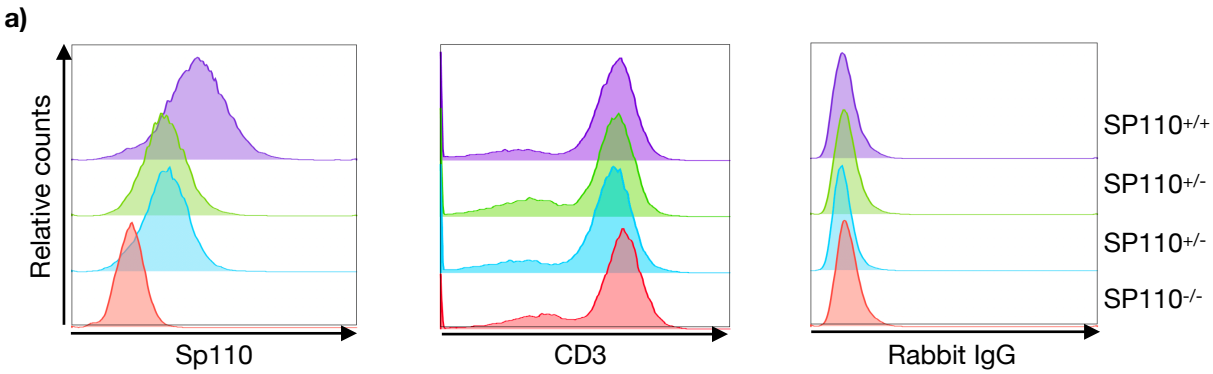

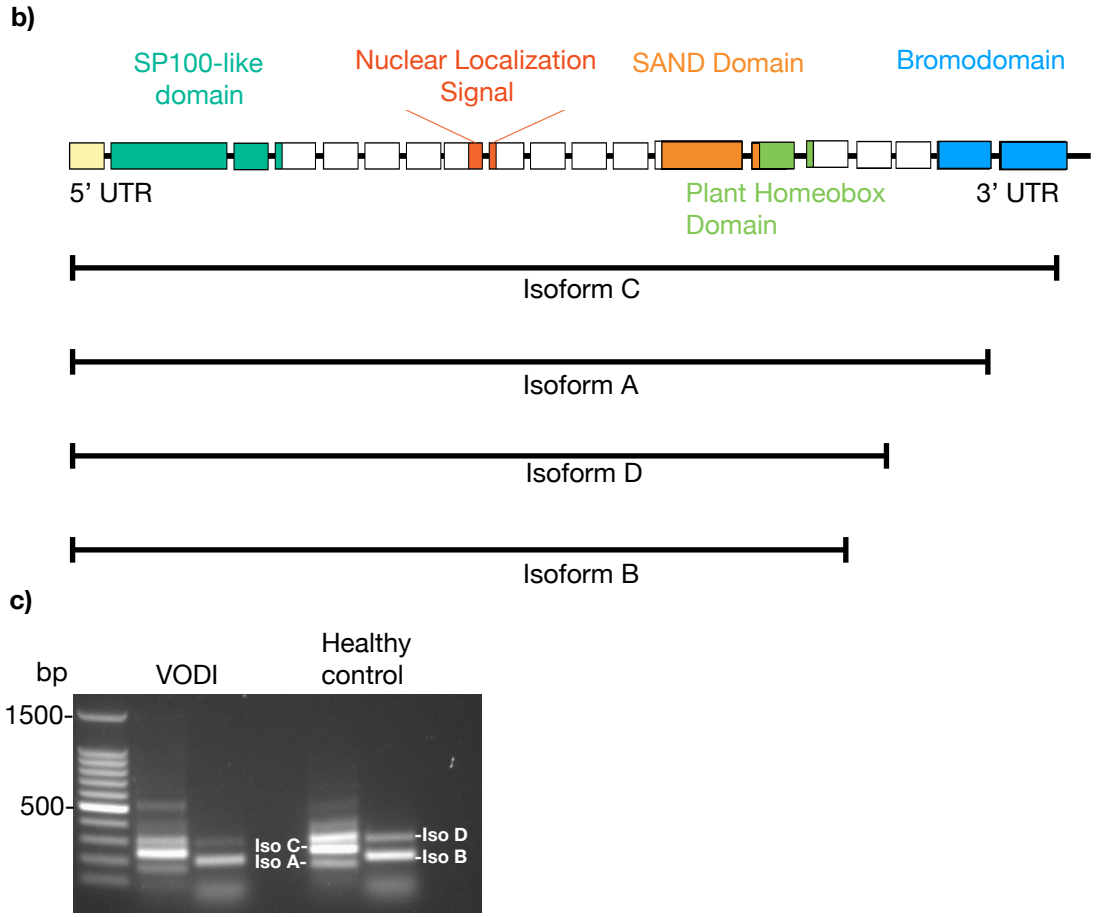

Figure 1

a) Sp110 protein expression in PBMC derived T cell blasts was assessed by flow cytometry in a VODI patient ($SP110^{-/-}$, patient nr. 3), two siblings carrying a disease-causing Sp110 mutation heterozygously ($SP110^{+/-}$) and a non-related control ($SP110^{+/+}$). Flow cytometric analysis of CD3-fluorescence or fluorescence following staining with normal rabbit IgG is depicted as a control. **b)** Schematic representation of the *SP110* gene. Lengths of the different isoforms are indicated. **c)** cDNA was generated from T cell blasts derived from a healthy individual or a VODI patient (patient nr. 1). Endpoint PCR analysis using specific primer amplifying either *SP110* isoform A and C (left lanes) or *SP110* isoforms B and D (right lanes) was performed and the different bands were visualized after agarose gel separation.

We next successfully generated a Jurkat T cell line lacking Sp110 expression ($SP110^{ko}$) using the CRISPR/Cas9 system (generation described in detail in [88]). Using the $SP110^{ko}$ Jurkat T cell line, we at next generated a Jurkat T cell line that stably overexpressed Sp110 ($SP110^{hi}$). To do this, we lentivirally transduced the $SP110^{ko}$ Jurkat T cell line with two different lentiviruses, either encoding for a *SP110* plus *GFP* ($SP110^{hi}$) or, as a transduction control, encoding for a *RFP* plus *GFP* ($SP110^{ko}$). *SP110* mRNA expression as tested by real-

time PCR was 20-fold higher in the SP110^{hi} and 3.5-fold higher in SP110^{wt} Jurkat T cells compared to *SP110* mRNA expression in SP110^{ko} Jurkat T cells (**Figure 2a**). Flow cytometric analysis of Sp110 expression revealed that, indeed, SP110^{hi} Jurkat T cells overexpressed Sp110 protein, while baseline Sp110 expression was observed in SP110^{wt} Jurkat T cells. In contrast, SP110^{ko} Jurkat T cells did not express Sp110. Staining with normal rabbit IgG was served as flow-cytometric staining control (**Figure 2b**).

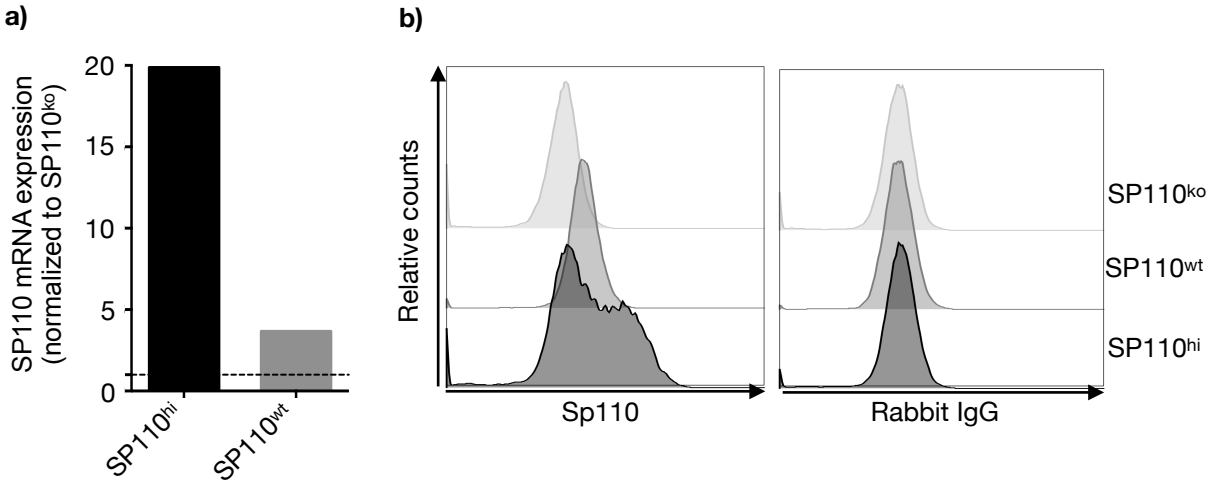

Figure 2

a+b) SP110^{ko}, SP110^{wt} and SP110^{hi} Jurkat T cells were analyzed for *SP110*/Sp110 expression. **a)** *SP110* mRNA expression was measured by real-time PCR in SP110^{ko}, SP110^{wt} and SP110^{hi} (expression in the latter was set to 1). **b)** Sp110 protein levels were measured by flow cytometry using Sp110-specific rabbit antiserum or normal rabbit IgG as a control (SP110^{ko} Jurkat T cells, light grey histograms; SP110^{wt} Jurkat T cells, dark grey histograms and SP110^{hi} Jurkat T cells, black histograms).

3.2 Analysis of T cell intrinsic roles of Sp110 that might support susceptibility to pneumocystis-induced disease in VODI patients

Pneumocystis is a typical opportunistic infection in patients chronically infected with HIV linked to the degree of CD4$^+$ T cell lymphopenia [91]. Although peripheral T cell numbers in VODI patients have been described to be within reference ranges for age [6], we used our cohort of VODI patients to determine the CD4$^+$/CD8$^+$ T cell ratio in PBMC and T cell blasts. As shown in **Figure 3a,** the CD4$^+$/CD8$^+$ T cell ratio was unaltered in PBMC from VODI

patients compared to healthy control individuals. There was no relative $CD4^+$ T cell lymphopenia that might have explained the susceptibility to pneumocystis. Also, following *in vitro* generation of T cell blasts derived from PBMC using PHA and IL-2 (see **methods**), the majority of T cell blasts were $CD8^+$ T cells, both in T cell blasts generated from VODI patients and from healthy control individuals (**Figure 3b**). Thus, we did not find evidence of differences in T cell subpopulations in VODI patients compared to healthy control individuals.

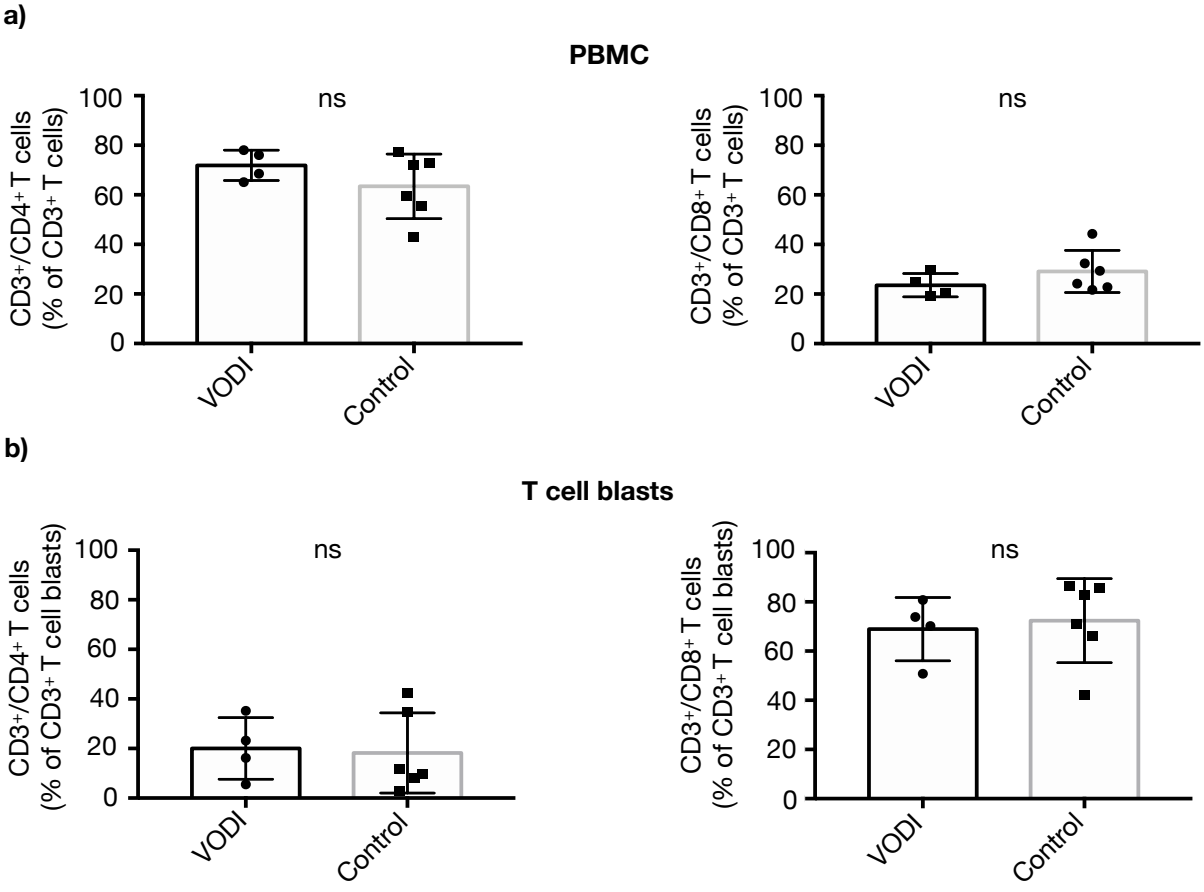

Figure 3

a+b) PBMC derived T cells or T cell blasts of VODI patients or healthy control individuals were stained for proteins defining the indicated T cell subsets and analyzed by flow cytometry. Statistics were performed with an unpaired T-test, ns = p>0,05; * = p<0,05; ** = p<0,005. Mean and standard deviation are depicted.

3.2.1 Sp110 orchestrates activation-induced T cell apoptosis

It has been convincingly demonstrated that T cell mediated immunopathology contributes to disease severity in pneumocystis infections [92]. In a murine pneumocystis infection model,

presence *vs.* absence of antibiotics against pneumocystis (Trimethoprim/Sulfamethoxazole) did not impact on survival, while *in vivo* depletion of T cells reduced mortality [84]. Activation-induced T cell apoptosis is a well-studied tightly regulated process to avoid T cell over-activity and immunopathology and to assure immune homeostasis [46].

We thus aimed to experimentally study whether T cell intrinsic Sp110 might impact on activation-induced T cell apoptosis and subsequently T cell mediated immunopathology following pneumocystis infection. Therefore, we *in vitro* re-stimulated Sp110 competent *vs.* deficient human T cell blasts with either the phorbol-ester PMA (known to activate immune signalling pathways downstream of the T cell receptor [93]), or induced apoptosis using an agonistic Fas (CD95)-specific antibody. Apoptosis was measured by AnnexinV staining and flow cytometric analysis. While both stimuli rapidly (within four hours) induced T cell apoptosis in Sp110 competent T cell blasts, a selective lack of apoptosis induction following PMA stimulation was repeatedly observed in T cell blasts derived from a VODI patient (patient nr. 1) (**Figure 4a**). While Fas-induced apoptosis was also slightly lower in T cell blasts derived from the VODI patient compared to T cell blasts from the two controls, the almost complete lack of PMA-induced apoptosis in Sp110 deficient T cell blasts was remarkable. Similarly, PMA failed to induce caspase-9 activation in T cell blasts derived from VODI patient nr. 1 while caspase-9 was activated in PMA re-stimulated Sp110 competent T cell blasts (**Figure 4b**). Thus, these results prompted us to study in more detail a potential role of Sp110 as a driver of activation-induced T cell death.

PMA has several limitations as a small molecule compound that induces T cell intrinsic signalling resulting in activation induced T cell apoptosis. First, as shown in **Figure 4c**, PMA induced apoptosis is augmented in T cell blasts generated from memory T cells when compared to T cell blasts generated from flow-sorted naïve PBMC derived T cells. This increased activation induced T cell apoptosis in memory T cells was also observed for anti-Fas treatment or TCR crosslinking with an agonistic anti-CD3 antibody (**Figure 4c** and data not shown). This finding is important to correct for when analysing human T cell blasts that consist of both naïve and memory T cell subpopulations. In addition, PMA failed to induce apoptosis in Jurkat T cells, even at concentrations that were 10-fold higher compared to PMA concentrations used to re-stimulate primary T cell blasts (**Figure 4d**). These results made PMA inappropriate as a compound to study activation induced apoptosis in $SP110^{ko}$ or $SP110^{hi}$ Jurkat T cells. In contrast, agonistic anti-Fas antibody induced apoptosis in Jurkat T cells comparably to primary T cell blasts (**Figure 4d**). While screening known inducers of T cell apoptosis, irradiation with UV-light was identified to induce dose-dependent apoptosis in both T cell blasts and Jurkat T cells (**Figure 4e+f**). In addition, flow-sorted naïve ($CD3^+CD27^+CD45RO^-$) or memory ($CD3^+CD27^-$) PBMC derived T cells displayed similar

apoptosis following UV-light irradiation (**Figure 4e**). Thus, UV-light irradiation proved to be the most useful apoptosis-inducing stimulus for subsequent experiments in primary T cell blasts and Jurkat T cells with absent, normal or exceeding Sp110 levels.

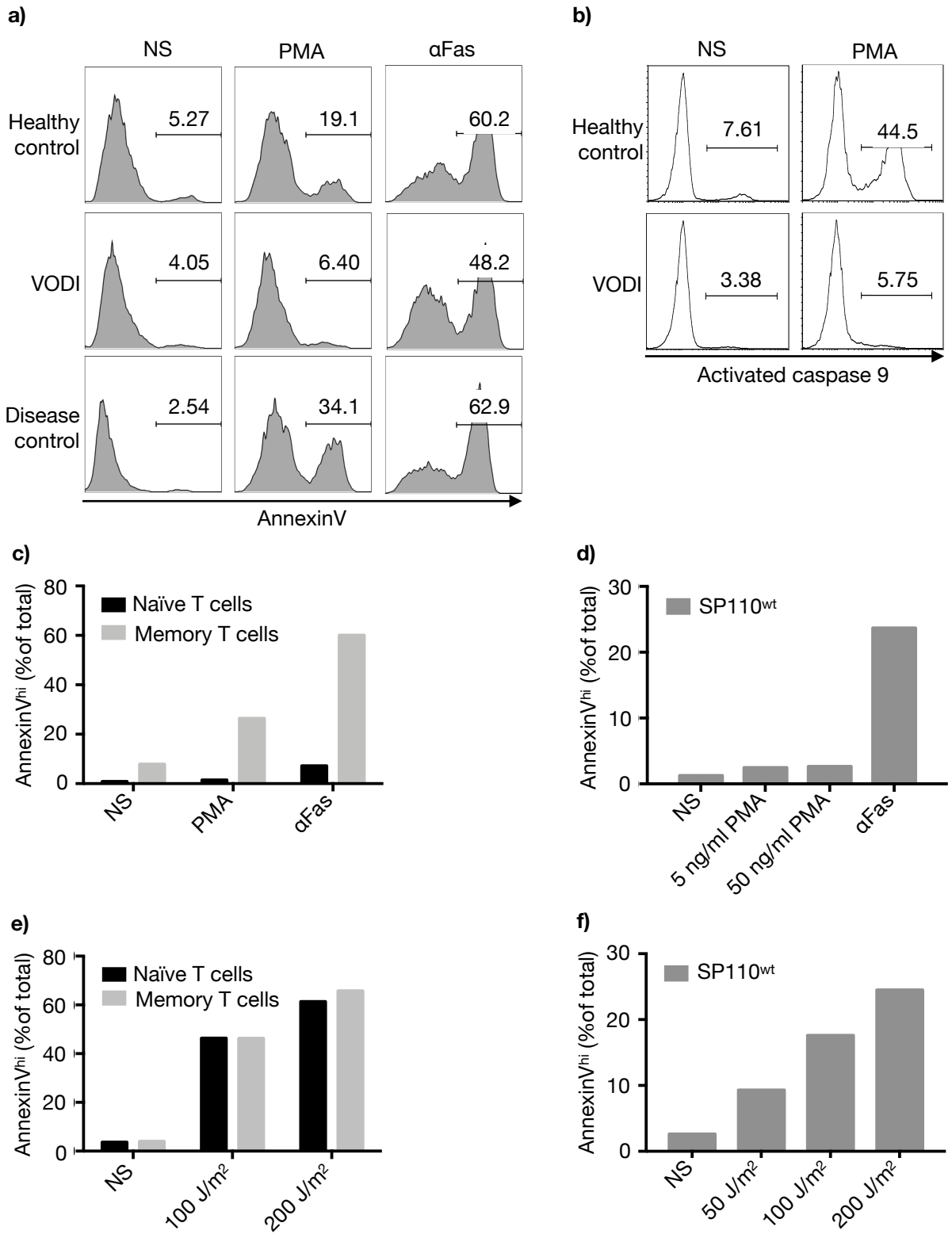

Figure 4

a+b) T cell blasts derived from a healthy control, a VODI patient (patient nr. 1) and a disease control patient (suffering from recurrent infections without evidence for immunodeficiency) were stimulated with either PMA or treated with agonistic anti-Fas antibody as indicated. **a)** Four hours later, T cell apoptosis was assessed by AnnexinV staining and flow cytometry. **b)** Activation of caspase-9 was measured by incubation of T cell blasts with fluorescently labelled caspase-9 inhibitor (FLICA) and flow cytometric analysis. **c)** T cell blasts generated from flow-sorted naïve ($CD3^+CD27^+CD45RO^-$) or memory ($CD3^+CD27^-$) PBMC derived T cells were stimulated using the indicated compounds. Apoptosis was assessed by AnnexinV staining and flow cytometry four hours later. **d)** $SP110^{wt}$ Jurkat T cells were stimulated with the indicated concentrations of PMA or treated with agonistic anti-Fas antibody and apoptosis was quantified by AnnexinV staining and flow cytometric analysis four hours later. **e)** T cell blasts were generated from flow-sorted naïve ($CD3^+CD27^+CD45RO^-$) *vs.* memory ($CD3^+CD27^-$) PBMC derived T cells and UV-light induced apoptosis was monitored using AnnexinV staining and flow cytometry. **f)** $SP110^{wt}$ Jurkat T cells were stimulated with the indicated intensities of UV-light. Four hours later, apoptosis was assessed using AnnexinV expression and flow cytometry.

PMA induced apoptosis in primary T cell blasts via the JNK/c-Jun signalling pathway, as apoptosis was blockable by pre-incubation with the JNK-specific inhibitor SP600125 [94] (**Figure 5a**). SP600125 similarly blocked UV-light induced apoptosis in primary T cell blasts and in Jurkat T cells (**Figure 5b**). Flow cytometric analysis of c-Jun serine phosphorylation at position 73 using phospho-specific c-Jun monoclonal antibody [95] emphasized that SP600125 pre-treatment indeed reduced c-Jun phosphorylation in primary T cell blasts and $SP110^{wt}$ Jurkat T cells (**Figure 5c**). PMA induced very low c-Jun phosphorylation in Jurkat T cells, probably explaining the lack of apoptosis induction in Jurkat T cells (data not shown). Thus, the JNK/c-Jun pathway is controlling PMA induced re-stimulation induced T cell apoptosis in primary T cell blasts and is orchestrating UV-light induced apoptosis in both primary T cell blasts and Jurkat T cells.

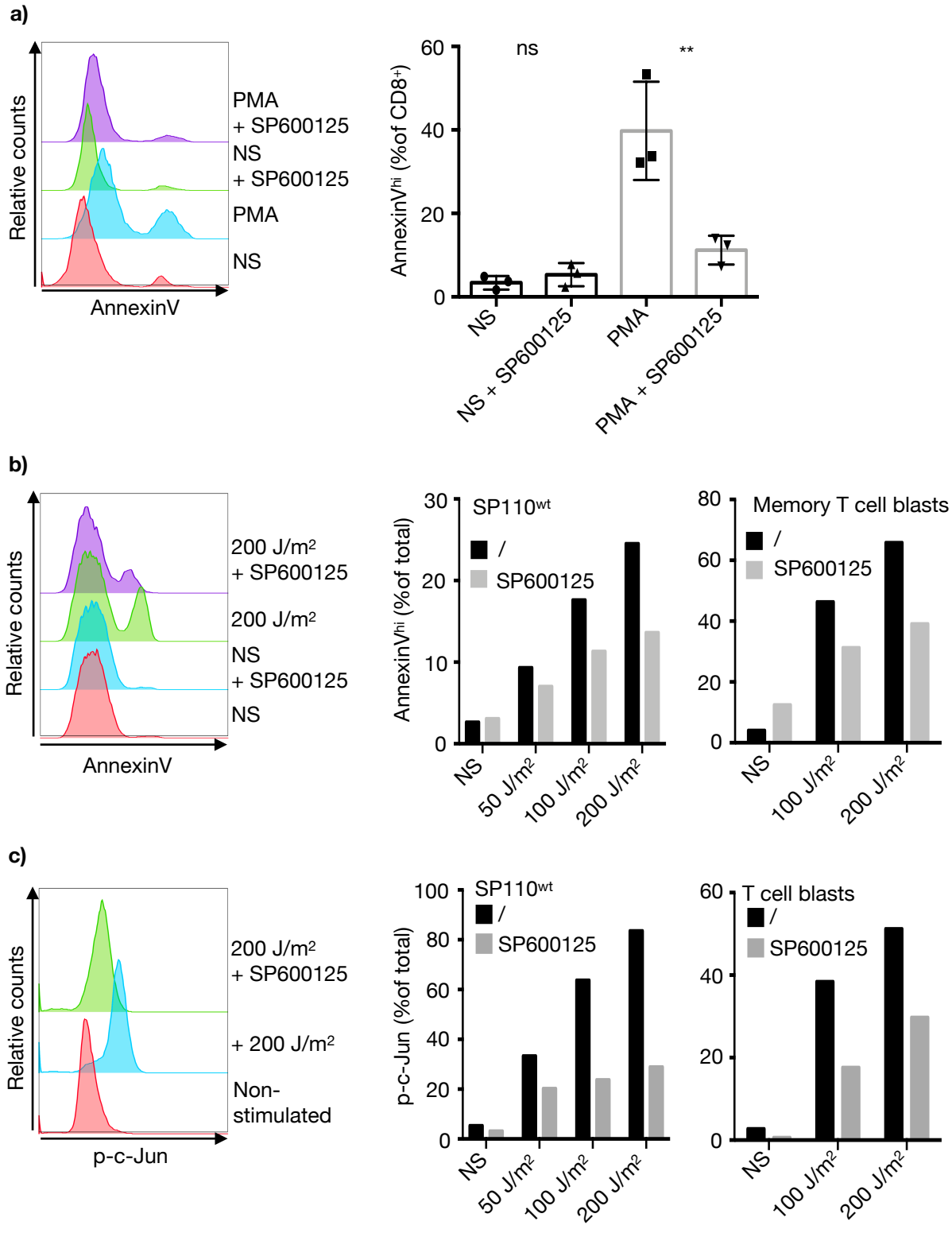

Figure 5

a) Primary T cell blasts were pre-incubated with the inhibitor SP600125 for 30 minutes or left untreated. Cells were then stimulated with PMA and apoptosis was quantified four hours later using AnnexinV staining and flow cytometric analysis. **b)** T cell blasts generated from flow-sorted memory

($CD3^+CD27^-$) PBMC derived T cells or $SP110^{wt}$ Jurkat T cells were irradiated with titrated intensities of UV-light. Apoptosis was assessed using AnnexinV staining and flow cytometric analysis four hours later. Pre-incubation with SP600125 for 30 minutes prior to UV-light irradiation served to block the JNK/c-Jun signaling pathway. **c)** Primary T cell blasts or $SP110^{wt}$ Jurkat T cells were pre-incubated with the c-Jun N-terminal kinase inhibitor SP600125 for 30 minutes and subsequently irradiated with titrated doses of UV-light. After one hour, the phosphorylation of c-Jun was assessed by phospho-flow cytometry. **a-c)** A representative histogram showing AnnexinV fluorescence is depicted in the left panel. Statistics were performed with an two-way ANOVA, ns = p>0,05; * = p<0,05; ** = p<0,005. Mean and standard deviation are depicted.

Since UV-light irradiation was identified as the most advantageous *in vitro* stimulus to study re-stimulation induced apoptosis in Jurkat T cells with varying expression levels of Sp110, we next UV-light irradiated $SP110^{wt}$ *vs.* $SP110^{hi}$ Jurkat T cells and analyzed apoptosis induction. Treatment with agonistic anti-Fas antibody served as a control. While Fas-induced apoptosis was similar in both cell lines, $SP110^{hi}$ Jurkat T cells displayed exaggerated apoptosis following UV-light irradiation compared to $SP110^{wt}$ Jurkat T cells (**Figure 6a**). In a separate, confirmatory experiment, $SP110^{ko}$, $SP110^{wt}$ and $SP110^{hi}$ Jurkat T cells were pre-incubated with the specific JNK inhibitor SP600125 or left untreated before irradiation with titrated doses of UV-light. Apoptosis induced by agonistic anti-Fas antibody served as a control. While T cell apoptosis was similar following anti-Fas treatment in all three cell lines, UV-light induced apoptosis correlated with Sp110 content, being highest in $SP110^{hi}$ and lowest in the $SP110^{ko}$ Jurkat T cells. UV-light induced, but not Fas-induced apoptosis was reduced by pre-incubation with the JNK inhibitor SP600125 (**Figure 6b**). In summary, Sp110 expression levels in Jurkat T cells correlated with augmented apoptosis subsequent to activation of the JNK/c-Jun pathway.

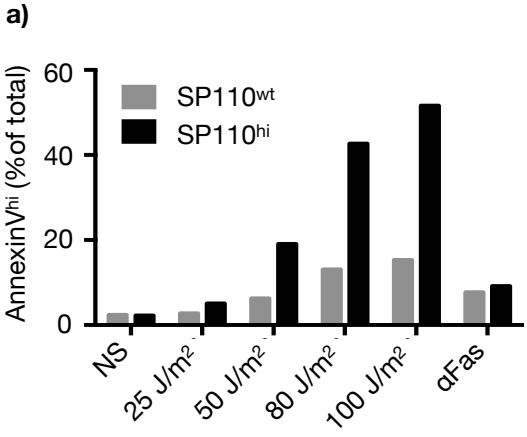

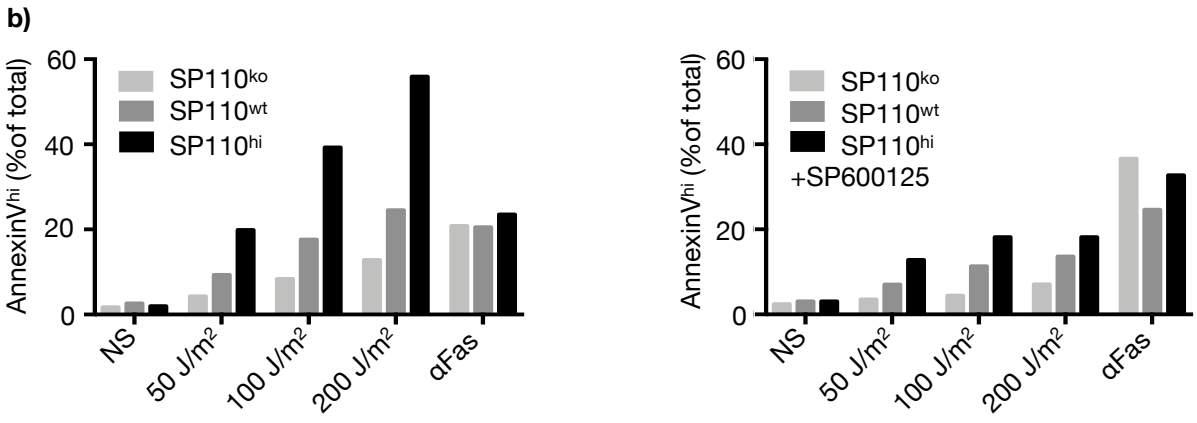

Figure 6

a) SP110^{wt} and SP110^{hi} Jurkat T cells were exposed to titrated intensities of UV-light or stimulated with an agonistic anti-Fas antibody. Four hours later, apoptosis was measured by flow cytometric quantification of AnnexinV binding. **b)** SP110^{ko}, SP110^{wt} and SP110^{hi} Jurkat T cells were irradiated with titrated intensities of UV-light or incubated with an agonistic anti-Fas antibody. Four hours later, T cell apoptosis was monitored by AnnexinV staining and flow cytometric analysis. As a control, cells were incubated for 30 minutes with SP600125 to block JNK/c-Jun signalling prior to UV-light irradiation or Fas cross-linking (right panel)

To confirm that the augmented UV-light induced apoptosis in SP110^{hi} Jurkat T cells was indeed due to the heightened Sp110 expression, we established *SP110* gene knockdown by transfection of SP110^{ko} and SP110^{hi} Jurkat T cells with *SP110* specific siRNA. Transfection with non-specific siRNA served as a control **(Figure 7a)**. Sp110 flow cytometric quantification 24 hours following transfection with *SP110* specific siRNA confirmed that Sp110 protein in SP110^{hi} Jurkat T cells was almost completely knocked-down (**Figure 7b**)**.** SP110^{ko} or SP110^{hi} Jurkat T cells were then UV-light irradiated and apoptosis was monitored four hours later. Treatment with agonistic anti-Fas antibody served as a control. Sp110 knockdown reduced UV-light induced apoptosis in SP110^{hi} Jurkat T cells by 50%, while it did not affect UV-light induced apoptosis in SP110^{ko} Jurkat T cells(**Figure 7c**). Fas-induced apoptosis was only slightly reduced by Sp110 knockdown in SP110^{hi} cells (**Figure 7c**). In summary, these experiments reassured the Sp110 driven augmentation of JNK/c-Jun related T cell apoptosis. They also suggested that Sp110 impacted on apoptosis pathways that are not centrally involved during Fas-related apoptosis.

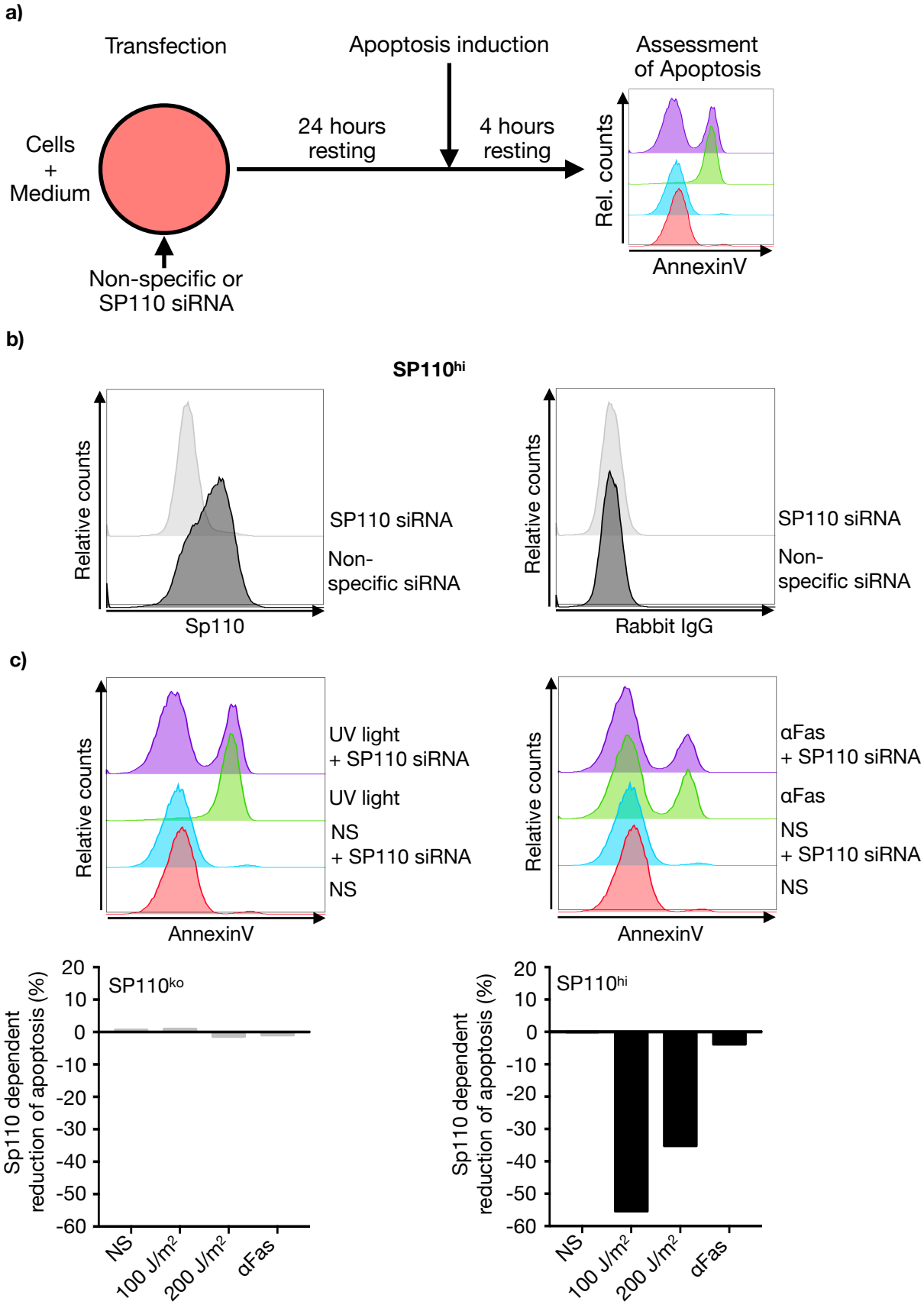
a)
Transfection
Apoptosis induction
Assessment of Apoptosis
Cells + Medium
24 hours resting
4 hours resting
Rel. counts
AnnexinV
Non-specific or SP110 siRNA
b)
SP110hi
Relative counts
SP110 siRNA
Non-specific siRNA
Sp110
Rabbit IgG
c)
UV light + SP110 siRNA
UV light
NS + SP110 siRNA
NS
αFas + SP110 siRNA
αFas
AnnexinV
SP110ko
SP110hi
Sp110 dependent reduction of apoptosis (%)
NS
100 J/m²
200 J/m²
αFas

Figure 7

a) A schematic graphical overview of the experiment is shown. **b)** SP110^{hi} Jurkat T cells were transfected with *SP110* specific (light grey histograms) or with non-specific siRNA (black histograms). 24 hours later, Sp110 protein expression was determined by flow cytometry. **c)** SP110^{ko} or SP110^{hi} Jurkat T cells were transfected with siRNA as shown in **a+b).** 24 hours later, Jurkat T cells were UV-light irradiated or incubated with agonistic anti-Fas antibody. Four hours later, apoptosis was quantified using AnnexinV staining and flow cytometric analysis. Representative histograms showing AnnexinV fluorescence in SP110^{hi} Jurkat T cells are depicted together with a summary graph showing relative apoptosis reduction following *SP110* siRNA transfection compared to transfection with non-specific siRNA.

3.2.1.1 T cell intrinsic Sp110 expression in T cells is regulated by interferon-α (IFN-I)

The nuclear body protein Sp110 has been described to be upregulated upon IFN stimulation in HL-60 leukemia cell lines [10]. To experimentally test whether also T cell intrinsic Sp110 levels are modified by IFN, SP110^{wt} Jurkats were stimulated with IFNα (IFN-I) for different time points. Incubation with IFN-I upregulated *SP110* mRNA levels in SP110^{wt} Jurkat T cells peaking at eight hours post-activation (**Figure 8a**). Sp110 protein upregulation peaked at 24 hours after IFN I stimulation in SP110^{wt} but not in SP110^{ko} Jurkat T cells, confirming that the increased flow cytometric Sp110 signal was indeed Sp110 specific (**Figure 8b**). In addition we stimulated primary T cell blasts derived from a healthy individual or a VODI patient (patient nr.1) with IFN-I. 24 hours later, Sp110 flow cytometric analysis revealed IFN-I mediated Sp110 upregulation in Sp110 competent but not in Sp110 deficient T cell blasts (**Figure 8b**). We next assessed, with the help of phospho-specific monoclonal antibodies, the IFN-I-induced phosphorylation of STAT1 [96] and 3 [97] by flow cytometry. IFN-I induced rapid phosphorylation of STAT1 and STAT3 similarly in SP110^{ko} and SP110^{wt} Jurkats showing that early IFN-I signalling occurred independently of presence *vs.* absence of Sp110 (**Figure 8c**). STAT phosphorylation could be blocked by pre-incubation with the panSTAT inhibitor SH-4-54 [98] for 30 min prior to IFN-I stimulation (**Figure 8c**). Pre-incubation with the panSTAT inhibitor SH-4-54 also precluded IFN-I mediated Sp110 upregulation in SP110^{wt} Jurkat T cells (**Figure 8c**). IFN-I activated SP110^{ko} Jurkat T cells served as a staining control (**Figure 8c**). Both, IFN-I driven STAT1 and STAT3 phosphorylation and IFN-I mediated upregulation of T cell intrinsic Sp110 protein levels could be similarly blocked by the JAK1/2 inhibitor Ruxolitinib [99] (**Figure 8d**). In summary, T cell intrinsic Sp110 levels, both in primary T cell

blasts and Jurkat T cells, are modified by IFN-I signals and are thus expected to be upregulated in inflamed tissues.

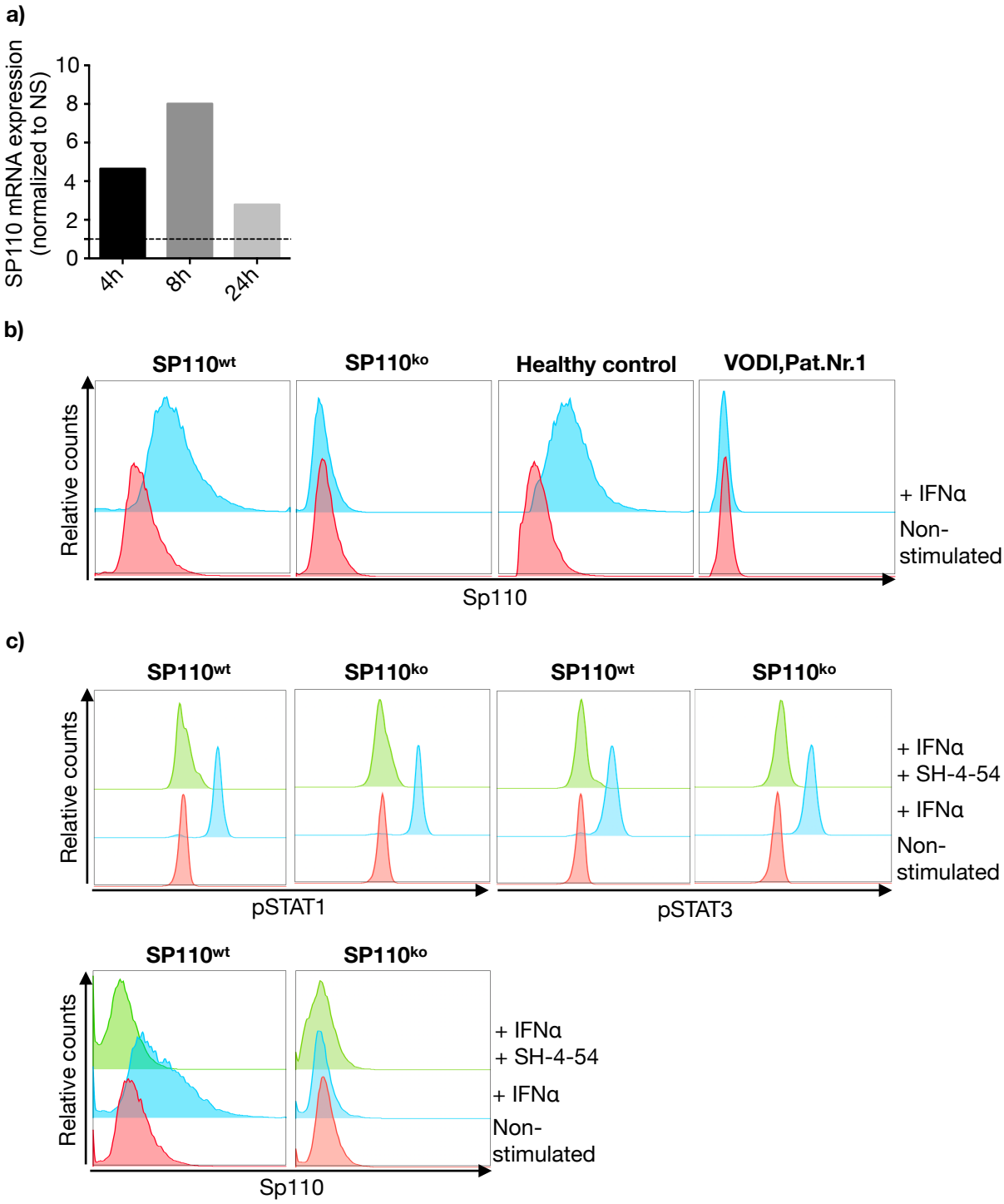

d)

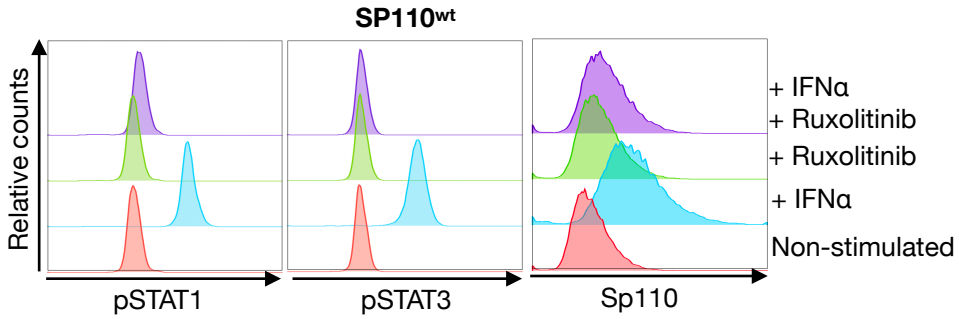

Figure 8

a) SP110^{wt} Jurkat T cells were stimulated with IFNα. At the indicated time points following IFNα stimulation, *SP110* mRNA expression was quantified by real-time PCR. Sp110 transcript levels under non-stimulated conditions were set to 1. **b)** SP110^{ko} and SP110^{wt} Jurkat T cells were stimulated with IFNα (blue histograms) or were left non-stimulated (red histograms). In addition, primary PBMC derived T cell blasts from a healthy control and a VODI patient (patient nr.1) were stimulated with IFNα or left unstimulated. 24 hours later, Sp110 protein levels were measured by flow cytometry **c)** SP110^{ko} and SP110^{wt} Jurkat T cells were treated with the panSTAT inhibitor SH-4-54 for 30 min prior to stimulation with IFNα for one hour. The phosphorylation of STAT1 and STAT3 was analyzed by staining with phospho-STAT1 and phospho-STAT3-specific antibodies and flow cytometric analysis. In addition, SP110^{ko} and SP110^{wt} Jurkat T cells were incubated with the panSTAT inhibitor SH-4-54 followed by IFNα stimulation. Sp110 expression was determined 24 hours later by flow cytometry. **d)** SP110^{wt} Jurkat T cells were incubated with the JAK1/2 inhibitor Ruxolitinib for 30 min or left without pre-incubation prior to stimulation with IFNα. One hour later, phosphorylation of STAT1 or STAT3 was measured using respective phospho-specific antibodies and flow cytometric analysis. Aliquots of similarly IFNα stimulated, Ruxolitinib pre-incubated SP110^{wt} Jurkat T cells were assessed 24 hours later for Sp110 protein expression by flow cytometry.

3.2.1.2 IFN-I stimulation functionally converts SP110^{wt} into SP110^{hi}, apoptosis-prone T cells

We hypothesized that IFN-I induced Sp110 upregulation might convert SP110^{wt} Jurkat T cells functionally into SP110^{hi}, apoptosis prone T cells. To experimentally study this, SP110^{wt} Jurkat T cells were transfected with *SP110* specific or non-specific siRNA and afterwards stimulated with IFN-I or left untreated for 24 hours. SP110^{wt} Jurkat T cells were then irradiated with titrated doses of UV-light and apoptosis was assessed four hours later (see graphical overview of the experiment in **Figure 9a**). Stimulation with agonistic anti-Fas served as a control. Analysis of Sp110 protein expression by flow cytometry reassured that

transfection with *SP110* specific siRNA completely blocked the IFN I driven Sp110 up-regulation in SP110^{wt} Jurkat T cells (**Figure 9b**). While Sp110 protein knockdown did not reduce UV-light induced apoptosis in SP110^{wt} Jurkat T cells, a knockdown of Sp110 protein in IFN-I stimulated SP110^{wt} Jurkat T cells reduced UV-light triggered apoptosis (**Figure 9c**). In other words, approximately 40% of UV-light (100 J/m^2) induced apoptosis in IFN-I activated SP110^{wt} Jurkat T cells occurred Sp110 dependently. These results were comparable to the Sp110 augmented apoptosis measured in SP110^{hi} Jurkat T cells following UV-light irradiation (**Figure 7**). Using the same experimental approach in primary human T cell blasts confirmed that Sp110 protein knockdown reduced UV-light induced apoptosis in IFN-I stimulated, but only minimally in non-activated T cell blasts. In contrast, only a small contribution of Sp110 to Fas-related apoptosis was observed (**Figure 9d**).

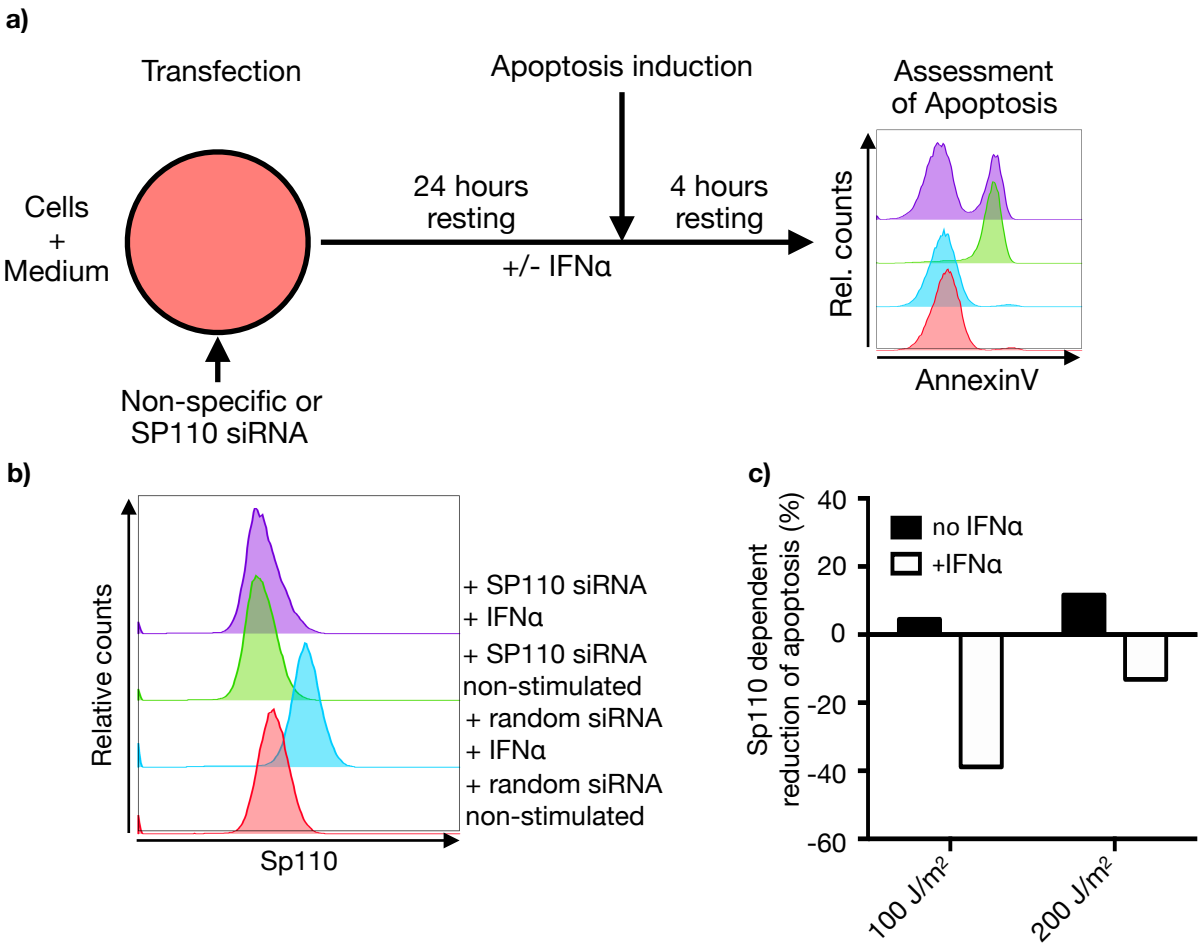

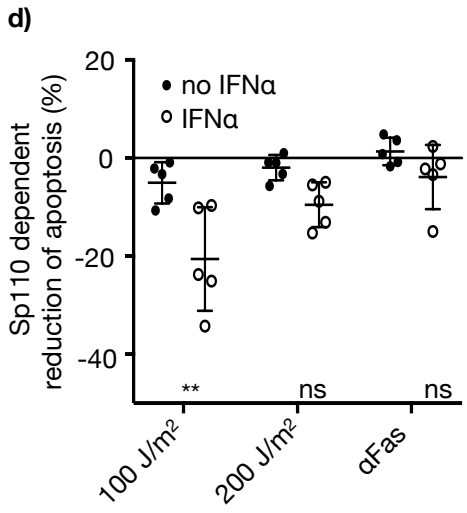

Figure 9

a) A schematic graphical overview of the experimental setup is depicted. **a-c)** SP110^{wt} Jurkat T cells were transfected with non-specific or *SP110* specific siRNA followed by stimulation with IFNα. Non-stimulated conditions served as a control. **b)** 24 hours later, Sp110 protein expression in T cells was quantified by flow cytometry. **a-c)** 24 hours following siRNA transfection, cells were irradiated with the indicated intensities of UV-light and apoptosis was measured four hours later by AnnexinV staining and flow cytometric analysis. The reduction of apoptosis in the absence *vs.* presence of Sp110 is depicted. **d)** Primary T cell blasts derived from healthy individuals were transfected with non-specific or *SP110* specific siRNA followed by stimulation with IFNα. Non-stimulated conditions served as a control. 24 hours later, T cell blasts were irradiated by the indicated doses of UV-light or incubated with agonistic anti-Fas antibody. Four hours later, apoptosis was measured by AnnexinV staining and flow cytometric analysis. The reduction of apoptosis in the absence *vs.* presence of Sp110 is depicted. Statistics were done with an two-way ANOVA, ns = p>0,05; * = p<0,05; ** = p<0,005. Mean and standard deviation are depicted.

3.2.1.3 Analysis of molecular mechanisms driving Sp110 dependent T cell apoptosis

Our previous results have shown that UV-light induced apoptosis both in primary T cell blasts and Jurkat T cells occurs JNK/c-Jun dependently (**Figure 5**). For this reason we next analyzed whether T cell intrinsic Sp110 levels impacted on phosphorylation of c-Jun following UV-light exposure. SP110^{wt} and SP110^{hi} Jurkat T cells were transfected with SP110 specific or non-specific siRNA and rested for 24 hours. Subsequently, Jurkat T cells were UV-light irradiated and one hour later the phosphorylation of c-Jun was assessed by phospho-flow cytometry. Phosphorylation of c-Jun occurred within one hour following UV-

light irradiation but was independently of Sp110 protein levels (**Figure 10a**). Thus, early UV-light induced T cell intrinsic signaling occurred independently of Sp110 protein levels. Next, we experimentally assessed whether UV-light induced apoptosis, which correlated with Sp110 expression levels, was affecting caspase-9 activation indicating activation of the *intrinsic* apoptosis pathway [100]. $SP110^{ko}$, $SP110^{wt}$ and $SP110^{hi}$ Jurkat T cells were irradiated with UV-light and cell lysates were preserved. Immunoblot analysis using a caspase-9 specific antibody demonstrated two proteolytically cleaved, caspase-9 bands, representing activated caspase-9 [101] at around 35-37 kDa besides non-activated full-length caspase-9 (50 kDa). Lysates generated from UV irradiated $SP110^{hi}$ Jurkat T cells revealed heightened caspase-9 activation (**Figure 10b**). Thus, UV-light irradiation induced T cell intrinsic, Sp110 augmented apoptosis correlating with enhanced activation of the *intrinsic* apoptosis pathway. Since *intrinsic* apoptosis is controlled by expression levels of proapoptotic BH3-only proteins such as NOXA, PUMA and BIM [61] [64], we next investigated transcriptional levels of the corresponding genes. $SP110^{ko}$, $SP110^{wt}$ and $SP110^{hi}$ Jurkat T cells were irradiated with UV-light. Four hours after UV-light irradiation of $SP110^{ko}$, $SP110^{wt}$ and $SP110^{hi}$ Jurkat T cells, cDNA was generated and the levels of *PUMA*, *NOXA* and *BIM* mRNA were quantified by real-time PCR. While UV-light induced *NOXA* and *BIM* expression did not correlate with Sp110 expression levels, we found a two-fold induction of *PUMA* mRNA in $SP110^{hi}$ but not in $SP110^{ko}$ and $SP110^{wt}$ Jurkat T cells following UV-light irradiation (**Figure 10c**). These results identified *PUMA* as a potential Sp110 regulated gene.

a)

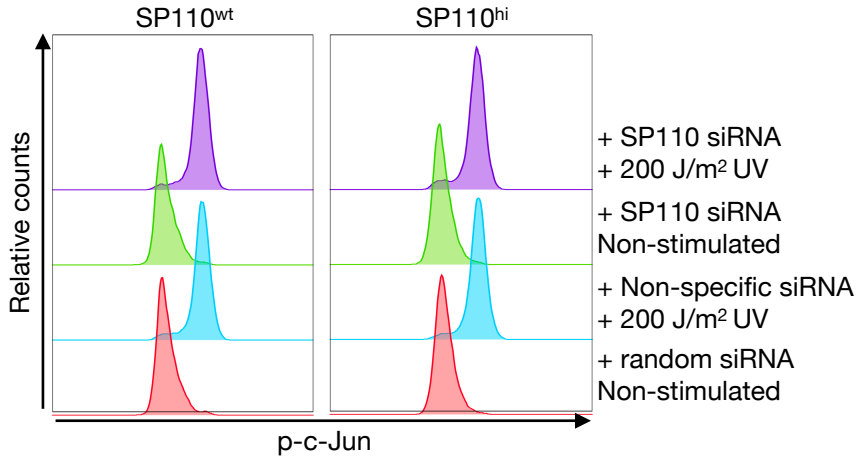

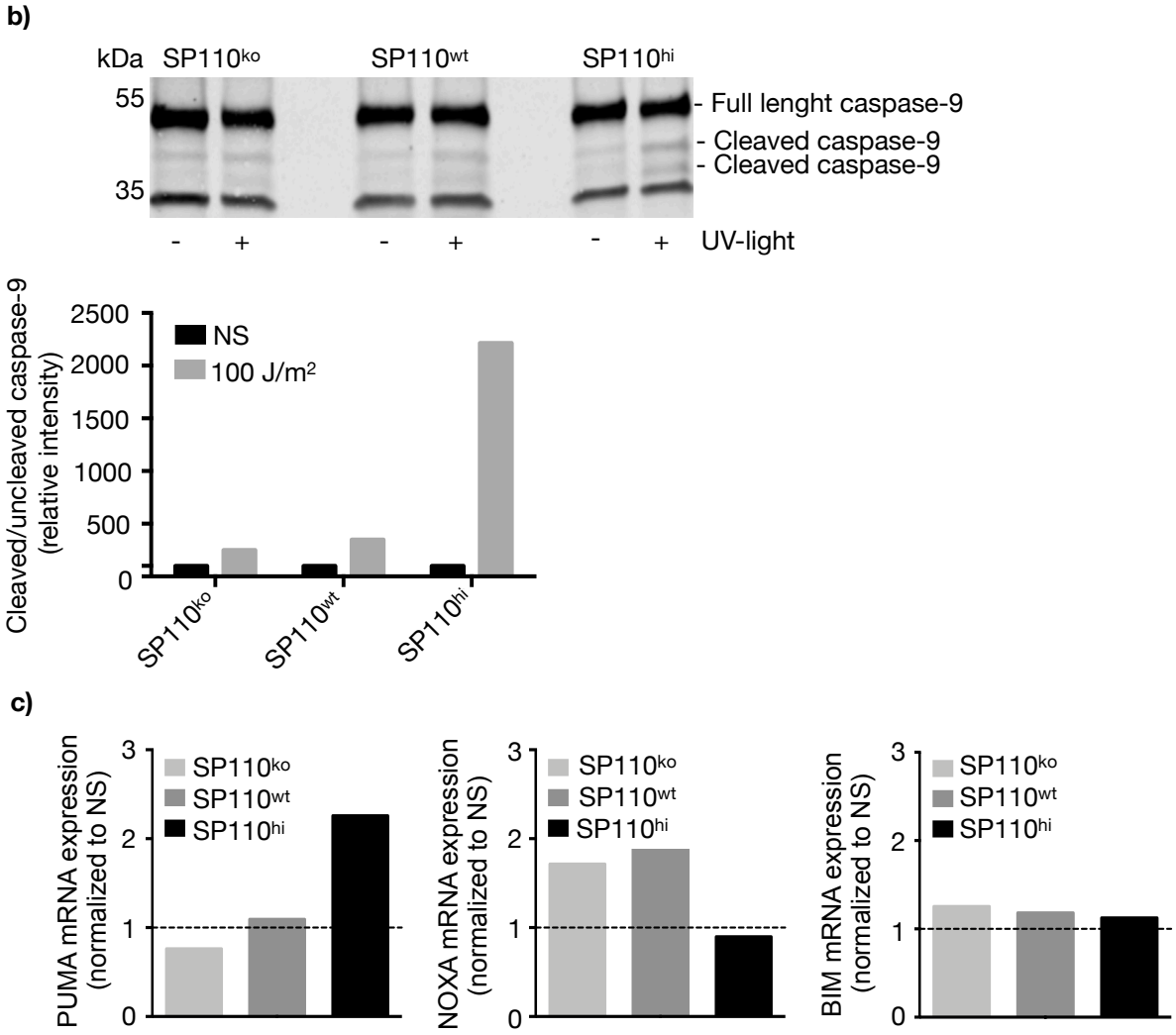

Figure 10

a) SP110^{wt} and SP110^{hi} Jurkat T cells were transfected with *SP110* specific or non-specific siRNA. 24 hours later the cells were stimulated by UV-light irradiation. One hour later, phosphorylation of c-Jun was determined by staining with a phospho-specific anti-c-Jun antibody and flow cytometric analysis. **b)** SP110^{ko}, SP110^{wt} and SP110^{hi} Jurkat T cells were irradiated with 100 J/m^2 UV-light. Four hours later, cellular lysates were analyzed by western blot for expression of full-length or activated, cleaved caspase-9 expression. A ratio of the signal intensities of cleaved caspase-9 to full-length caspase-9 was calculated and is depicted (left panel). The ratio of the signal intensities of cleaved caspase-9 over full-length caspase-9 in non-stimulated SP110^{ko} Jurkat T cells was arbitrarily set to 1. **c)** SP110^{ko}, SP110^{wt} and SP110^{hi} Jurkat T cells were irradiated with UV-light (100 J/m^2). Four hours later, cDNA was generated and the expression of *PUMA*, *NOXA* or *BIM* was quantified by real-time PCR. The mRNA expression was normalized to mRNA levels of the indicated gene measured in the respective Jurkat T cells in the absence of UV-light stimulation.

3.2.1.4 Sp110 driven T cell apoptosis does not require expression of the full bromodomain

The bromodomain of Sp110 is thought to play an important role for its transcriptional function [22]. To experimentally test whether expression of the full-length Sp110 isoform encoding a complete bromodomain is required for Sp110 augmented T cell apoptosis, two different Jurkat T cell lines overexpressing the truncated *SP110* isoform A were generated by lentiviral transduction. Both $SP110^{iso\text{-}A}$ Jurkat T cell lines overexpressed *SP110* four-fold as measured by real-time PCR compared to $SP110^{wt}$ Jurkat T cells (data not shown). Endpoint PCR analysis using primer amplifying all four SP110 isoforms (see **Figure 1c**) revealed that $SP110^{wt}$ Jurkat T cells primarily expressed the full-length *SP110* isoform C (Iso C) whereas the $SP110^{iso\text{-}A}$ Jurkat T cell lines expressed particularly the truncated *SP110* isoform A (Iso A) (**Figure 11a**). When the different Jurkat T cell lines were irradiated with titrated amounts of UV-light, both $SP110^{hi}$ and $SP110^{iso\text{-}A}$ Jurkat T cell lines displayed augmented apoptosis induction compared to $SP110^{wt}$ Jurkat T cells. Fas-induced apoptosis was similar in all tested Jurkat T cell lines (**Figure 11b**). In a separate set of experiments, we confirmed that UV-light induced apoptosis, also in $SP110^{iso\text{-}A}$ Jurkat T cells, occurred via the JNK/c-Jun pathway, as it was blockable by pre-incubation with the JNK specific inhibitor SP600125 (**Figure 11c**). In summary, these data suggested that Sp110 driven JNK/c-Jun dependent apoptosis did not require expression of a full bromodomain.

a)

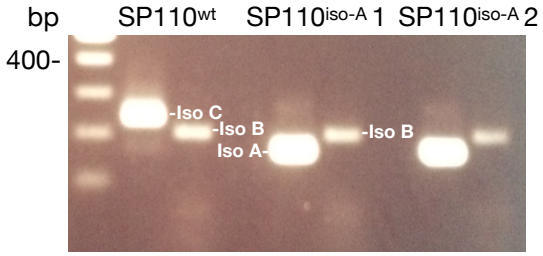

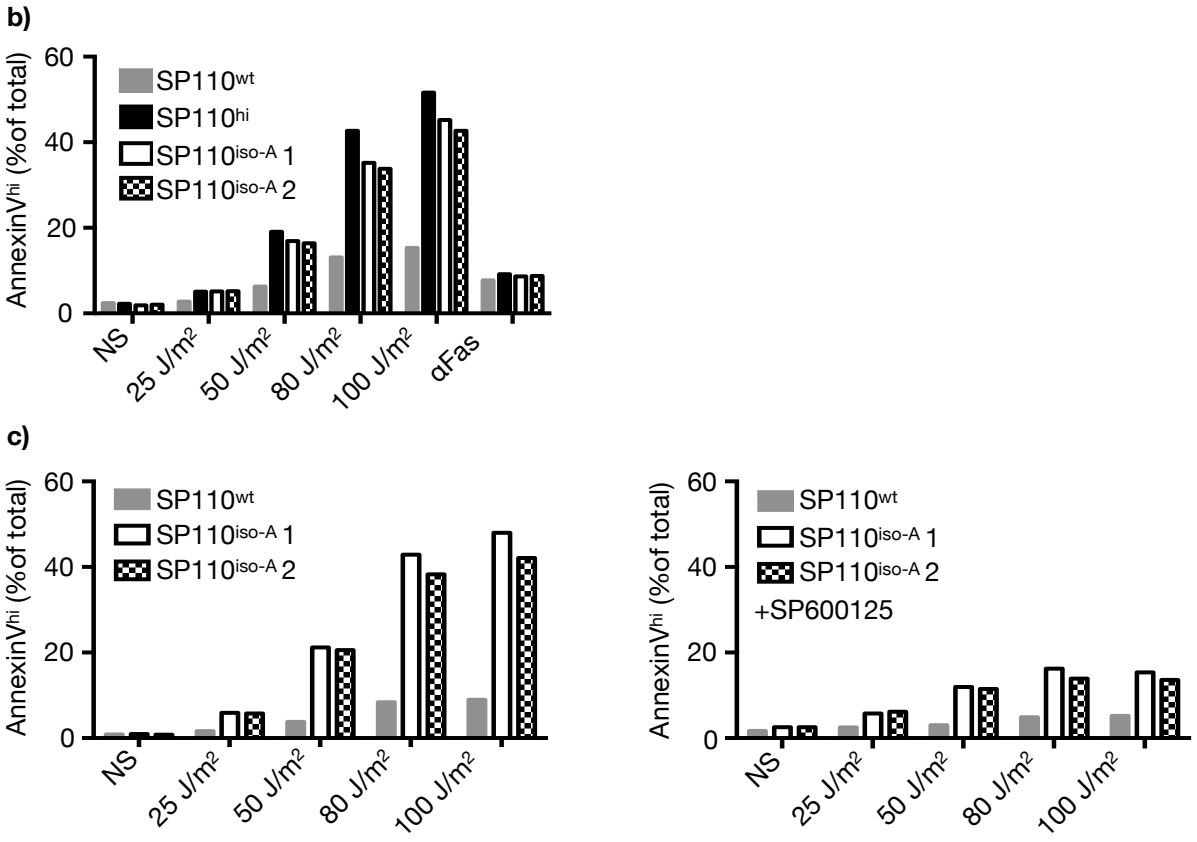

Figure 11

a) cDNA of the indicated Jurkat T cell lines was generated and endpoint PCR specific for the indicated *SP110* isoforms was performed. Specific bands were visualized following agarose gel separation. **b)** SP110^{wt} and two SP110^{iso-A} Jurkat T cell lines were irradiated with titrated doses of UV-light or stimulated with an agonistic anti-Fas antibody. Four hours later, apoptosis was assessed by AnnexinV staining and flow cytometric analysis. **c)** SP110^{wt} and two SP110^{iso-A} Jurkat T cell lines were irradiated with titrated doses of UV-light in the absence *vs.* presence of the JNK/c-Jun specific inhibitor SP600125. Four hours later, Jurkat T cell apoptosis was measured by AnnexinV staining and flow cytometric analysis.

3.2.2 T cell intrinsic IFN-γ production is regulated by Sp110 expression

While impaired activation induced apoptosis may support T cell mediated immunopathology, uncontrolled excess T cell-intrinsic cytokine production has also been linked to immunopathological disease, exemplarily shown in hemophagocytic lymphohistiocytosis (HLH) [102]. We therefore experimentally addressed the question whether presence *vs.* absence of Sp110 in T cells might regulate production of T cell specific cytokines. SP110^{ko}, SP110^{wt} and SP110^{hi} Jurkat T cells were stimulated with UV-light and upregulation of IFNγ

mRNA was assessed by real-time PCR four hours later. IFNγ mRNA was 30-fold increased following UV-light stimulation in SP110^{ko} Jurkat T cells, while upregulation was 4 - 6-fold lower in Sp110 competent Jurkat T cells. In contrast, TNFα mRNA was only minimally induced following UV-light irradiation in all Jurkat T cell lines tested (**Figure 12a**). To confirm that absence of Sp110 induced excess T cell intrinsic IFNγ formation, we transfected SP110^{wt} Jurkat T cells with *SP110 vs.* non-specific siRNA followed by stimulation with IFN-I for 24 hours. Afterwards cells were UV-light irradiated and IFNγ mRNA levels were quantified by real-time PCR four hours later. Sp110 knockdown was associated with excess UV-light driven IFNγ mRNA levels, particularly in IFN-I activated SP110^{wt} Jurkat T cells (**Figure 12b**).

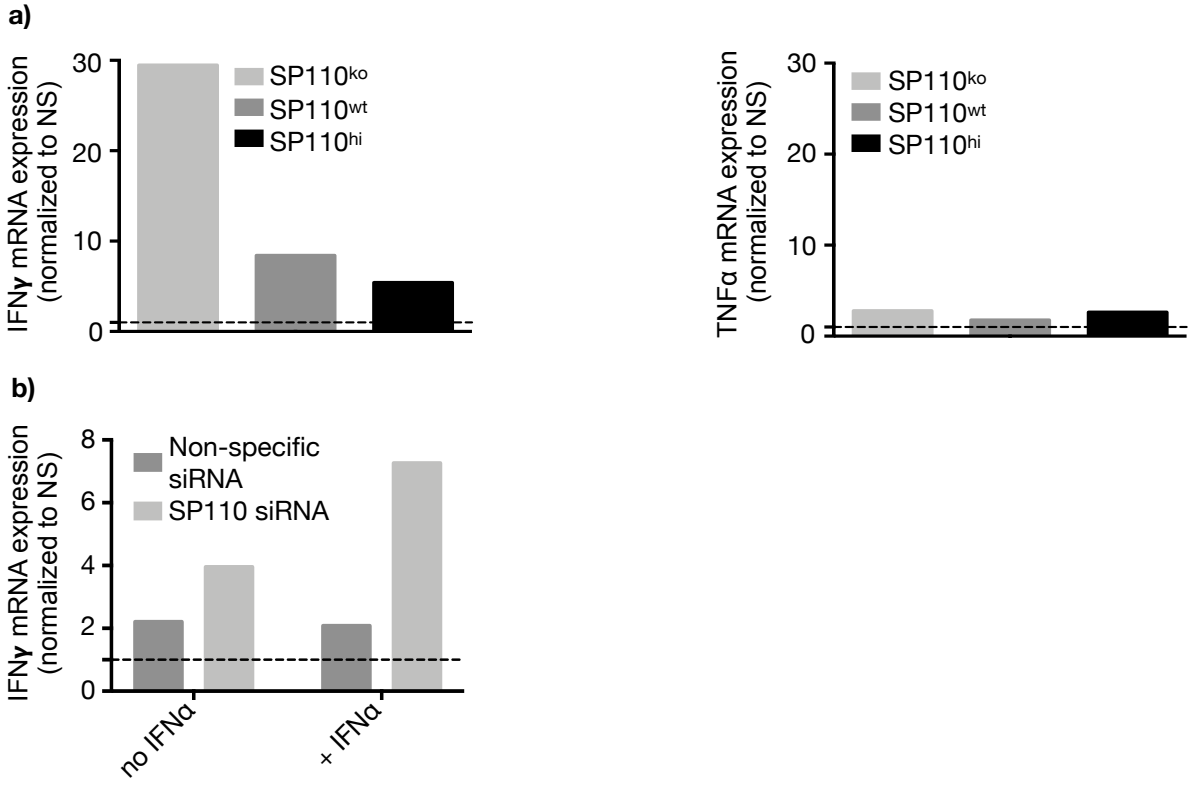

Figure 12

a) SP110^{ko}, SP110^{wt} and SP110^{hi} Jurkat T cells were irradiated with UV-light (100J/m^2). Four hours later, cDNA was generated and IFNγ or TNFα transcripts were quantified by real-time PCR. The fold-increase compared transcript levels measured in non-stimulated cells (set to 1) is depicted. **b)** SP110^{wt} Jurkat T cells were transfected with *SP110* specific or non-specific siRNA as indicated, followed by stimulation with IFN-I. Non-stimulated conditions served as a control. 24 hours later, Jurkat T cells were irradiated with UV-light (100J/m^2) or left non-irradiated and *IFNγ* mRNA was assessed by real-time PCR four hours later. IFNγ transcript levels are depicted relative to levels measured in non-irradiated conditions (set to 1).

4 Discussion

4.1 Flow-cytometric detection of T cell intrinsic Sp110 to screen for veno-occlusive disease with immunodeficiency (VODI) and other potential clinical applications

The diagnosis of veno-occlusive disease with immunodeficiency has been challenging, as it was mainly based on genetic detection of rare *SP110* mutations already known to cause VODI. The testing of functional consequences of novel *SP110* mutations has until now been virtually impossible since no functional Sp110 dependent immune-assays have been described. As part of my PhD thesis we have established the flow-cytometric detection of Sp110 protein quantity in peripheral blood derived human T cells. This novel flow-cytometry based method has been recently published by *Marquardsen and Baldin et al in the Journal of Clinical Immunology* allowing to rapidly screen patients for potential VODI [88]. A not yet published modification of this diagnostic test is to apply Sp110 flow-cytometric quantification in PBMC derived T cells following *in vitro* IFN-I stimulation *vs.* non-stimulated conditions. As IFN-I treatment increases T cell intrinsic Sp110 expression, the advantage of this modification is that the Sp110 signal difference between Sp110 competent *vs.* deficient T cells is increasing, thereby augmenting the sensitivity of the diagnostic test. In addition, *in vitro* IFN-I stimulation prior to Sp110 flow-cytometric analysis allows functional testing of normal Sp110 regulation by IFN-I. This would allow to identify Sp110 deficient patients with e.g. mutations in the *SP110* promotor that would not be diagnosed when performing exon-based Sanger sequencing or whole exome sequencing.

Besides VODI, the flow cytometric analysis of Sp110 allows to functionally characterize single nucleotide variants (SNP) in the *SP110* gene and their respective impact on Sp110 expression. It also remains to be tested whether specific *SP110* SNP associate with T cell apoptosis or IFNγ production.

As Sp110 is an IFN-stimulated protein, the flow-cytometric quantification of Sp110 could also have a diagnostic role to detect diseases associated with increased IFN-I responses. Interferonopathies are monogenic PID due to gain of function mutations in genes regulating IFN-I formation [103]. These diseases often manifest as autoimmune diseases [42]. In addition, polygenetic diseases such as systemic lupus erythematosus (SLE) or chronic virus infections are linked to enhanced IFN production [42 104]. The detection of exaggerated IFN-I production by ELISA has been proven difficult [105]. Monitoring Sp110 levels by flow-cytometry in peripheral blood derived cells may be used as a biomarker of the clinical activity of these

diseases and their response to immune-modulating treatment.

4.2 Sp110 as a regulator of JNK/c-Jun dependent T cell apoptosis

Overexpression of T cell intrinsic Sp110 augmented UV-light induced apoptosis both in primary human T cell blasts and Jurkat T cells. Since phosphorylation of c-Jun as assessed by flow-cytometry occurred independently of Sp110 protein levels, we hypothesize that Sp110 may alter c-Jun dependent gene-regulation in the nucleus. Sp110 is guided to the nucleus via its NLS whereas c-Jun is transported to the nucleus via a specific nuclear import receptor [10 106]. c-Jun phosphorylation is not required for nuclear import [107]. Indeed, c-Jun has been demonstrated to associate with PML, which, like Sp110, is member of the family of PML nuclear body proteins [108]. The association of PML with c-Jun requires c-Jun phosphorylation [108]. It thus seems reasonable to hypothesize that phosphorylated c-Jun directly interacts with Sp110 and as a consequence of this induces altered gene transcription. We are currently experimentally testing whether Sp110 and p-c-Jun co-localize following UV-light irradiation using immunofluorescence imaging and immunoprecipitation techniques.

Although we have mainly studied UV-light induced T cell apoptosis, we believe that our results are relevant for T cell apoptosis induced via T cell receptor (TCR) crosslinking. In support of this, T cells from JNK1-deficient mice have been demonstrated to display reduced activation induced T cell apoptosis following TCR ligation [109]. In addition, activation induced T cell apoptosis of melanoma-specific or influenza-specific T cells upon interaction with cognate peptide has been demonstrated to occur JNK dependently [110 111 112]. We have shown that both PMA stimulation and TCR cross-linking by agonistic anti-CD3 antibody induced phosphorylation of c-Jun, with similar kinetics compared to UV-light irradiation (data not shown). It is noteworthy, that irradiation activates similar signalling pathways as TCR cross-linking [113]. Besides the rather selective activation of the JNK/c-Jun signalling pathway following UV-light irradiation, TCR cross-linking will simultaneously activate a broader range of signalling pathways, including the NF-κB pathway, which might impact on c-Jun dependent apoptosis [114].

Some proapoptotic BH-3 only proteins such as NOXA, PUMA and BIM are transcriptionally regulated and represent thus interesting candidates as potentially Sp110 regulated proteins [115]. Together with NOXA, PUMA favours MOMP by activating the proapoptotic BCL-2 family members BAK and BAX [63 65]. Our results demonstrate that upon UV-light irradiation of Jurkat

T cells, *PUMA* mRNA increase was highest in Jurkat T cells overexpressing Sp110. In contrast, no such Sp110 dependent effect was observed for *NOXA* or *BIM* mRNA expression. Still, this association has not yet been shown to be causal for the increased Sp110 dependent apoptosis augmentation. Experiments are planned to analyse whether augmented apoptosis induced by Sp110 overexpression is reduced by siRNA mediated knock down of *PUMA* expression. A more unbiased approach would be to transfect $SP110^{hi}$ Jurkat T cells or IFN-stimulated primary human T cell blasts with *SP110* specific siRNA and compare the UV-light induced transcriptome with T cells transfected with non-specific siRNA. In addition, chromatin immunoprecipitation DNA-sequencing (ChIP-seq) experiments will help to define potential Sp110 regulated genes.

4.3 Regulation of UV-light induced T cell apoptosis by different Sp110 isoforms

The nuclear body protein Sp110 contains different functional domains, including a bromodomain at the C-terminus of the protein (also see **Figure 1b**) [10]. This domain is thought to be important for the transcriptional activity of Sp110 [22]. A very recent study from *Leu et al* showed that different Sp110 isoforms have specific functions regarding the regulation of gene expression. The middle region and the C-terminal part of *SP110* are regulating the cellular localization of the protein. Besides the NLS, this study reported that the Sp110 SAND and bromodomain are essential for correct nuclear targeting [23]. Our results showed that all four main *SP110* isoforms are expressed in primary human T cell blasts from healthy individuals. We have not yet assessed the T cell intrinsic expression compartment of the different Sp110 isoforms, but this could be achieved by overexpression of selected Sp110 isoforms in $SP110^{ko}$ Jurkat T cells followed by immunofluorescence microscopy or western blot analysis of lysates of enriched subcellular compartments.

However, we have experimentally demonstrated that overexpression of *SP110* isoform A, lacking parts of the bromodomain, similar to overexpression of the full length isoform C, augmented UV-light induced, JNK/c-Jun dependent apoptosis. This suggests that the missing bromodomain part in isoform A is dispensable for Sp110 augmented apoptosis. Similar functional analyses in Jurkat T cells overexpressing the other Sp110 isoforms will allow to better defining required protein domains for the apoptosis-enhancing functions of Sp110.

4.4 The role of IFN-I in Sp110 augmented apoptosis, immunopathology and immune dysregulation

Sp110 is an interferon stimulated protein [10]. Our results imply that a certain level of Sp110 protein is required to mediate Sp110 augmented T cell apoptosis. This critical threshold of Sp110 expression is higher compared to basal levels found at steady state in both primary human T cell blasts and Jurkat T cells but is reached in both cell types following IFN-I stimulation *in vitro*. In other words, IFN-I increases Sp110 to levels where Sp110 dependent apoptosis augmentation is observed. Bringing these findings into a clinical context it is likely that Sp110 augmented T cell apoptosis occurs primarily in inflamed tissues where IFN-I production mainly occurs, such as e.g. in the lung during pneumocystis infection. The experimental evidence that Sp110 does not control activation induced T cell apoptosis at steady state would easily explain why Sp110 deficiency does not lead to altered T cell homeostasis in the absence of infection. The immune-biologic correlate of this are the normal numbers of T cells and the absence of lymphoproliferation (splenomegaly and/or lymphadenopathy) in patients with VODI [6]. In contrast, during pneumocystis infection of immunologically healthy individuals, local IFN-I levels would rise and enhance Sp110 levels to a threshold where activation induced T cell apoptosis is augmented, thus prohibiting immunopathological lung damage. This proposed mechanism is not specific for pneumocystis and would apply similarly for other infections that are linked to immunopathology. Notably, T cell mediated immunopathology has been postulated in murine and human CMV infections which are known to induce life-threatening disease in VODI patients [116] [117] [118] [86]. Besides its essential role in the pathogenesis of VODI, Sp110 augmented apoptosis might also play a role in other diseases that are associated with enhanced IFN-I or ISG-signature. These consist of the rare above-mentioned interferonopathies leading to enhanced or uncontrolled ISG activation due to monogenic mutations in genes controlling IFN-I formation [42]. More frequent, polygenic systemic autoimmune diseases such as SLE or chronic viral infections such as HIV are linked to exaggerated IFN-I production [119] [120]. These states of IFN-I overproduction, based on our proposed mechanism, would be associated with enhanced T cell apoptosis. Indeed, T cell lymphopenia is a typical hallmark of both SLE and HIV [121] [91].

Further studies are planned to experimentally test the hypothesis that in these autoimmune or chronic virus replication-associated diseases, IFN-I driven Sp110 overexpression would drive T cell apoptosis and thus contribute to T cell lymphopenia.

4.5 Sp110 dependent regulation of T cell intrinsic IFN-γ production

IFNγ is a key effector cytokine produced by activated T cells [122]. It is essential for the control of intracellular pathogens such as mycobacteria [123]. On the other hand, uncontrolled or excess IFNγ production is known to be the cause for immunopathology. This has been exemplarily shown in HLH where uncontrolled IFNγ causes immunopathologic disease that is associated with high mortality [102]. In fact, biologics targeting IFNγ are currently used in clinical trials to treat immunopathologic diseases [124]. T cell-dependent immunopathology is also a hallmark of pneumocystis pneumonia [125] [126]. The mechanisms how IFNγ enhances immunopathology are pleiotropic including, amongst others, macrophage activation, upregulation of MHC molecules and thus augmentation of antigen presentation and increased attraction of cytotoxic $CD8^+$ T cells into the inflamed area which further augments IFN-γ formation [127] [128] [129].

Our experiments demonstrate that absence of Sp110 expression was associated with augmented *IFNγ* mRNA levels following UV irradiation of Jurkat T cells. If control experiments confirm this regulatory function of Sp110 also in primary human T cells, we have identified a previously unknown immune-regulatory function of Sp110.

In VODI patients, both, the identified Sp110 dependent effect on T cell apoptosis on one hand and the regulation of IFNγ production on the other hand are altered. During pneumocystis infection, this would result in activated T cells that displaying impaired activation-induced apoptosis in inflamed tissue while secreting uncontrolled amounts of IFNγ. This might explain the special susceptibility to severe pneumocystis infections in VODI patients. A graphical summary assembling all identified Sp110 dependent T cell intrinsic functions and their relation to T cell immunopathology during pneumocystis infection are depicted in **Figure 13**.

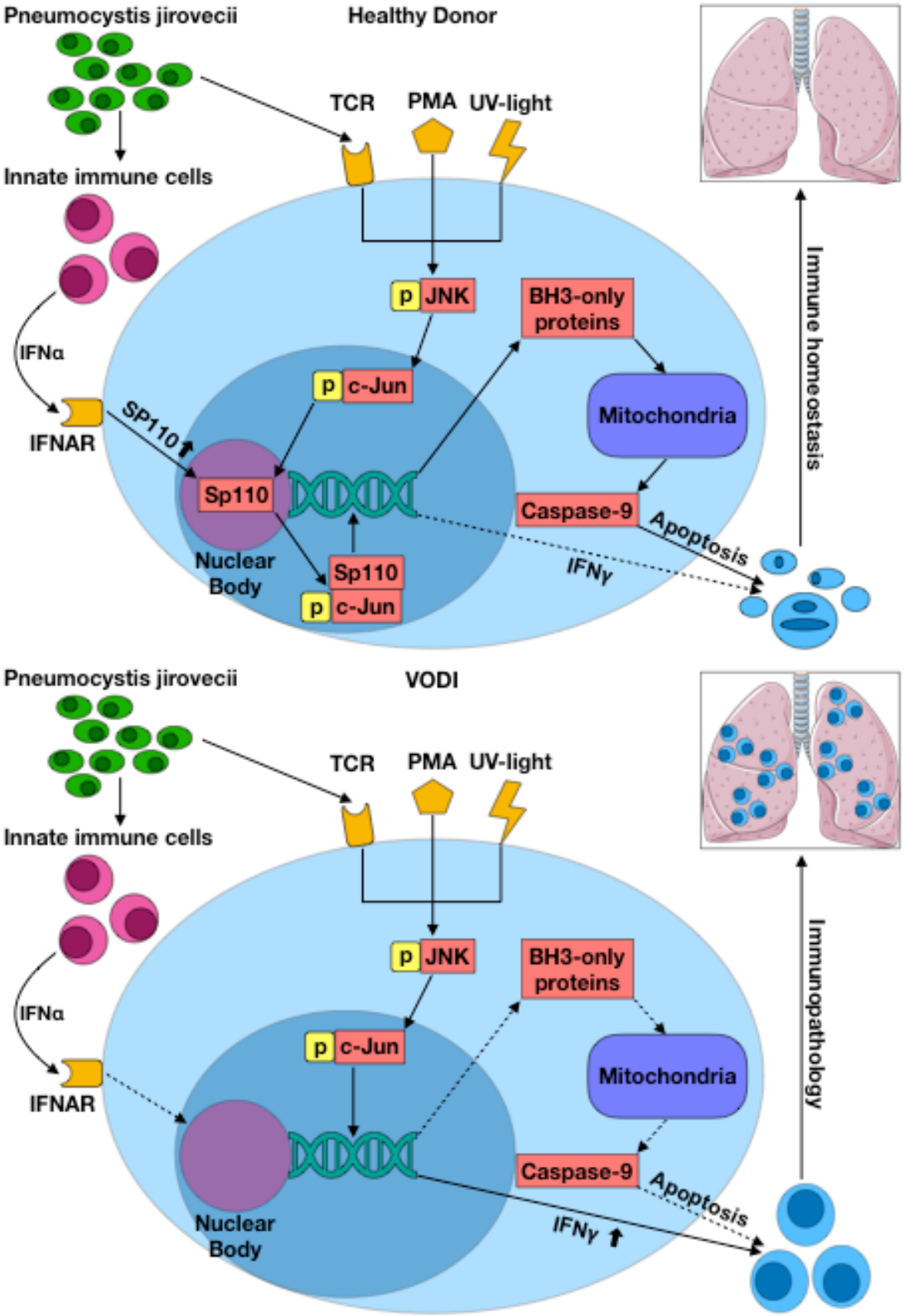

Figure 13 Lung picture was copied from https://smart.servier.com

5 References

1. Rezaei, N., Aghamohammadi, A. & Notarangelo, L. D. Primary immunodeficiency diseases: Definition, Diagnosis and Management. *Springer Berlin Heidelb. GmbH Co. K.* (2017).

2. Picard, C. *et al.* International Union of Immunological Societies: 2017 Primary Immunodeficiency Diseases Committee Report on Inborn Errors of Immunity. *J. Clin. Immunol.* **38,** 96–128 (2018).

3. Van Der Burg, M. & Gennery, A. R. Educational paper: The expanding clinical and immunological spectrum of severe combined immunodeficiency. *Eur. J. Pediatr.* **170,** 561–571 (2011).

4. Mellis, C. & Bale, P. M. Familial hepatic venoocclusive disease with probable immune deficiency. *J. Pediatr.* **88,** 236–242 (1976).

5. Roscioli, T., Ziegler, J. B., Buckley, M. & Wong, M. Hepatic Veno-Occlusive Disease with Immunodeficiency. (2017).

6. Roscioli, T. *et al.* Mutations in the gene encoding the PML nuclear body protein Sp110 are associated with immunodeficiency and hepatic veno-occlusive disease. *Nat. Genet.* **38,** 620–622 (2006).

7. Grunebaum, E. *et al.* Bone marrow transplantation for severe combined immune deficiency. *JAMA* **295,** 508–518 (2006).

8. Ganaiem, H. *et al.* The role of hematopoietic stem cell transplantation in SP110 associated veno-occlusive disease with immunodeficiency syndrome. *Pediatr. Allergy Immunol.* **24,** 250–256 (2013).

9. Brasch, K. & Ochs, R. Nuclear Bodies (NBs): A Newly 'Rediscoveres' Organelle. **223,** 211–223 (1992).

10. Bloch, D. B. *et al.* Sp110 localizes to the PML-Sp100 nuclear body and may function as a nuclear hormone receptor transcriptional coactivator. *Mol. Cell. Biol.* **20,** 6138–6146 (2000).

11. Fagioli, M. *et al.* Cooperation between the RING + B1-B2 and coiled-coil domains of PML is necessary for its effects on cell survival. *Oncogene* **16,** 2905–2913 (1998).

12. Zhong, S., Salomoni, P. & Pandolfi, P. P. The transcription role of PML and the

nuclear body. *Nat. Cell Biol.* **2,** 85–90 (2000).

13. Wang, Z. G. *et al.* Pml is essential for multiple apoptotic pathways. *Nat. Genet.* **20,** 266–272 (1998).

14. Fusconi, M. *et al.* Anti-nuclear antibodies of primary biliary cirrhosis recognize 78–92-kD and 96–100-kD proteins of nuclear bodies. *Clin. Exp. Immunol.* **83,** 291–297 (1991).

15. Evans, J., Reuben, A. & Craft, J. Pbc 95K, a 95-Kilodalton nuclear autoantigen in primary biliary cirrhosis. *Arthritis Rheum.* 1–6 (1991).

16. Szostecki, C., Will, H., Netter, H. J. & Guldner, H. H. Autoantibodies to the nuclear Sp100 protein in primary biliary cirrhosis and associated diseases: epitope specificity and immunoglobulin class distribution. *Scand. J. Immunol.* **36,** 555–564 (1992).

17. Bloch, D. B., De la Monte, S. M., Guigaouri, P., Filippov, A. & Bloch, K. D. Identification and characterization of a leukocyte-specific component of the nuclear body. *J. Biol. Chem.* **271,** 29198–29204 (1996).

18. Seeler, J. S., Marchio, a, Sitterlin, D., Transy, C. & Dejean, a. Interaction of SP100 with HP1 proteins: a link between the promyelocytic leukemia-associated nuclear bodies and the chromatin compartment. *Proc. Natl. Acad. Sci. U. S. A.* **95,** 7316–7321 (1998).

19. Gibson, T. J., Ramu, C., Gemũnd, C. & Aasland, R. The APECED polyglandular autoimmune syndrome protein, AIRE-1, contains the SAND domain and is probably a transcription factor [1]. *Trends Biochem. Sci.* **23,** 242–244 (1998).

20. Bottomley, M. J. *et al.* The SAND domain structure defines a novel DNA-binding fold in transcriptional regulation. *Nat. Struct. Biol.* **8,** 626–633 (2001).

21. Bienz, M. The PHD finger, a nuclear protein-interaction domain. *Trends Biochem. Sci.* **31,** 35–40 (2006).

22. Sanchez, R. & Zhou, M.-M. The role of human bromodomains in chromatin biology and gene transcription. *Curr. Opin. Drug Discov. Devel.* **12,** 659–65 (2009).

23. Leu, J. S., Chang, S. Y., Mu, C. Y., Chen, M. L. & Yan, B. S. Functional domains of SP110 that modulate its transcriptional regulatory function and cellular translocation. *J. Biomed. Sci.* **25,** 1–15 (2018).

24. Abhimanyu, Jha, P., Jain, A., Arora, K. & Bose, M. Genetic association study suggests

a role for SP110 variants in lymph node tuberculosis but not pulmonary tuberculosis in north Indians. *Hum. Immunol.* **72,** 576–580 (2011).

25. Fox, G. J. *et al.* Polymorphisms of SP110 are associated with both pulmonary and extra-pulmonary tuberculosis among the Vietnamese. *PLoS One* **9,** (2014).

26. Jiang, S.-Y. *et al.* The effects of SP110's associated genes on fresh cavitary pulmonary tuberculosis in Han Chinese population. *Clin. Exp. Med.* **16,** 219–225 (2016).

27. Thye, T. *et al.* No associations of human pulmonary tuberculosis with Sp110 variants. *Journal of medical genetics* **43,** e32 (2006).

28. Png, E. *et al.* Polymorphisms in SP110 are not associated with pulmonary tuberculosis in Indonesians. *Infect. Genet. Evol.* **12,** 1319–1323 (2012).

29. Pan, H. *et al.* Ipr1 gene mediates innate immunity to tuberculosis. *Nature* **434,** 767–772 (2005).

30. Nikpour, M., Dempsey, A. A., Urowitz, M. B., Gladman, D. D. & Barnes, D. A. Association of a gene expression profile from whole blood with disease activity in systemic lupus erythaematosus. *Ann. Rheum. Dis.* **67,** 1069–1075 (2008).

31. Alizadeh, A. *et al.* Distinct types of primary cutaneous large B-cell lymphoma identi ed by gene expression pro ling. *Gene Expr.* **105,** 3671–3678 (2009).

32. Rosenwald, A. *et al.* After Chemotherapy for Diffuse Large-B-Cell Lymphoma. *N. Engl. J. Med.* **346,** 1937–1947 (2015).

33. Yan, N. & Chen, Z. J. Intrinsic antiviral immunity. *Nat. Immunol.* **13,** 214–222 (2012).

34. Pestka, S., Krause, C. D. & Walter, M. R. Interferons, interferon-like cytokines, and their receptors. *Immunol. Rev.* **202,** 8–32 (2004).

35. Isaacs, A. & Lindemann, J. Virus interference. I. The interferon. *Proc. R. Soc. London. Ser. B, Biol. Sci.* **147,** 258–267 (1957).

36. Isaacs, A., Lindenmann, J. & Valentine, R. C. Pillars Article: Virus Interference. II. Some Properties of Interferon. Proc R Soc Lond B Biol Sci. 1957. 147: 268-273. *J. Immunol.* **195,** 1921–1926 (2015).

37. Majer, O. *et al.* Type I interferons promote fatal immunopathology by regulating inflammatory monocytes and neutrophils during Candida infections. *PLoS Pathog.* **8,** e1002811 (2012).

38. de Weerd, N. A., Samarajiwa, S. A. & Hertzog, P. J. Type I interferon receptors: biochemistry and biological functions. *J. Biol. Chem.* **282,** 20053–20057 (2007).

39. Uze, G., Schreiber, G., Piehler, J. & Pellegrini, S. The receptor of the type I interferon family. *Curr. Top. Microbiol. Immunol.* **316,** 71–95 (2007).

40. Decker, T., Muller, M. & Stockinger, S. The yin and yang of type I interferon activity in bacterial infection. *Nat. Rev. Immunol.* **5,** 675–687 (2005).

41. Martin, S. J., Finucane, D. M., Amarante-Mendes, G. P., O'Brien, G. A. & Green, D. R. Phosphatidylserine externalization during CD95-induced apoptosis of cells and cytoplasts requires ICE/CED-3 protease activity. *J. Biol. Chem.* **271,** 28753–28756 (1996).

42. Lee-Kirsch, M. A. The Type I Interferonopathies. *Annu. Rev. Med.* **68,** 297–315 (2017).

43. Hall, J. C. & Rosen, A. Type I interferons: crucial participants in disease amplification in autoimmunity. *Nat. Rev. Rheumatol.* **6,** 40–49 (2010).

44. Jouanguy, E. *et al.* Human primary immunodeficiencies of type I interferons. *Biochimie* **89,** 878–883 (2007).

45. Galluzzi, L. *et al.* Essential versus accessory aspects of cell death: recommendations of the NCCD 2015. *Cell Death Differ.* **22,** 58–73 (2015).

46. Arens, R. *et al.* Cutting edge: CD95 maintains effector T cell homeostasis in chronic immune activation. *J. Immunol.* **174,** 5915–5920 (2005).

47. Galluzzi, L. *et al.* Molecular mechanisms of cell death: recommendations of the Nomenclature Committee on Cell Death 2018. *Cell Death Differ.* **25,** 486–541 (2018).

48. Locksley, R. M., Killeen, N. & Lenardo, M. J. The TNF and TNF Receptor Superfamilies. *Cell* **104,** 487–501 (2001).

49. Ashkenazi, A. & Dixit, V. Death Receptors : Signaling and Modulation. **281,** 1305–1308 (1998).

50. Peter, M. & Krammer, P. Mechanisms of CD95 (APO-1/Fas)- mediated apoptosis. *Curr Opin Immunol* **10,** 545–51 (1998).

51. Suliman, A., Lam, A., Datta, R. & Srivastava, R. K. Intracellular mechanisms of TRAIL: Apoptosis through mitochondrial-dependent and -independent pathways. *Oncogene* **20,** 2122–2133 (2001).

52. Schall, T. J. *et al.* Molecular cloning and expression of a receptor for human tumor necrosis factor. *Cell* **61,** 361–370 (1990).

53. Peter, M. E. & Krammer, P. H. The CD95(APO-1/Fas) DISC and beyond. *Cell Death Differ.* **10,** 26–35 (2003).

54. Schleich, K. *et al.* Stoichiometry of the CD95 Death-Inducing Signaling Complex: Experimental and Modeling Evidence for a Death Effector Domain Chain Model. *Mol. Cell* **47,** 306–319 (2012).

55. Barnhart, B. C., Alappat, E. C. & Peter, M. E. The CD95 type I/type II model. *Semin. Immunol.* **15,** 185–193 (2003).

56. Elmore, S. Apoptosis: a review of programmed cell death. *Toxicol. Pathol.* **35,** 495–516 (2007).

57. Tait, S. W. G. & Green, D. R. Mitochondria and cell death: outer membrane permeabilization and beyond. *Nat. Rev. Mol. Cell Biol.* **11,** 621–632 (2010).

58. Czabotar, P. E., Lessene, G., Strasser, A. & Adams, J. M. Control of apoptosis by the BCL-2 protein family: Implications for physiology and therapy. *Nat. Rev. Mol. Cell Biol.* **15,** 49–63 (2014).

59. Luna-Vargas, M. P. A. & Chipuk, J. E. Physiological and Pharmacological Control of BAK, BAX, and Beyond. *T rends Cell Biol.* **155,** 3–12 (2017).

60. Llambi, F. *et al.* BOK Is a Non-canonical BCL-2 Family Effector of Apoptosis Regulated by ER-Associated Degradation. *Cell* **165,** 421–433 (2016).

61. Villunger, A. *et al.* p53- and drug-induced apoptotic responses mediated by BH3-only proteins puma and noxa. *Science* **302,** 1036–1038 (2003).

62. Dai, H., Pang, Y.-P., Ramirez-Alvarado, M. & Kaufmann, S. H. Evaluation of the BH3-only protein Puma as a direct Bak activator. *J. Biol. Chem.* **289,** 89–99 (2014).

63. Chen, H.-C. *et al.* An interconnected hierarchical model of cell death regulation by the BCL-2 family. *Nat. Cell Biol.* **17,** 1270–1281 (2015).

64. Ren, D. *et al.* BID, BIM, and PUMA are essential for activation of the BAX- and BAK-dependent cell death program. *Science* **330,** 1390–1393 (2010).

65. Li, M. X. *et al.* BAK alpha6 permits activation by BH3-only proteins and homooligomerization via the canonical hydrophobic groove. *Proc. Natl. Acad. Sci. U. S. A.* **114,** 7629–7634 (2017).

66. Kim, H. *et al.* Stepwise activation of BAX and BAK by tBID, BIM, and PUMA initiates mitochondrial apoptosis. *Mol. Cell* **36,** 487–499 (2009).

67. Grosse, L. *et al.* Bax assembles into large ring-like structures remodeling the mitochondrial outer membrane in apoptosis. *EMBO J.* **35,** 402–413 (2016).

68. Aluvila, S. *et al.* Organization of the mitochondrial apoptotic BAK pore: oligomerization of the BAK homodimers. *J. Biol. Chem.* **289,** 2537–2551 (2014).

69. Moldoveanu, T., Follis, A. V., Kriwacki, R. W. & Green, D. R. Many players in BCL-2 family affairs. *Trends Biochem. Sci.* **39,** 101–111 (2014).

70. Llambi, F. *et al.* A unified model of mammalian BCL-2 protein family interactions at the mitochondria. *Mol. Cell* **44,** 517–531 (2011).

71. Tait, S. W. G. & Green, D. R. Mitochondrial regulation of cell death. *Cold Spring Harb. Perspect. Biol.* **5,** (2013).

72. Liu, X., Kim, C. N., Yang, J., Jemmerson, R. & Wang, X. Induction of apoptotic program in cell-free extracts: requirement for dATP and cytochrome c. *Cell* **86,** 147–157 (1996).

73. Li, P. *et al.* Cytochrome c and dATP-dependent formation of Apaf-1/caspase-9 complex initiates an apoptotic protease cascade. *Cell* **91,** 479–489 (1997).

74. Julien, O. & Wells, J. A. Caspases and their substrates. *Cell Death Differ.* **24,** 1380–1389 (2017).

75. Shalini, S., Dorstyn, L., Dawar, S. & Kumar, S. Old, new and emerging functions of caspases. *Cell Death Differ.* **22,** 526–539 (2015).

76. Nagata, S. DNA degradation in development and programmed cell death. *Annu. Rev. Immunol.* **23,** 853–875 (2005).

77. Coleman, M. L. *et al.* Membrane blebbing during apoptosis results from caspase-mediated activation of ROCK I. *Nat. Cell Biol.* **3,** 339–345 (2001).

78. Sebbagh, M. *et al.* Caspase-3-mediated cleavage of ROCK I induces MLC phosphorylation and apoptotic membrane blebbing. *Nat. Cell Biol.* **3,** 346–352 (2001).

79. Frenkel, J. K. Pneumocystis pneumonia, an immunodeficiency-dependent disease (IDD): a critical historical overview. *J. Eukaryot. Microbiol.* **Volume: 46,** (1999).

80. Edman, J. C. *et al.* Ribosomal RNA sequence shows Pneumocystis carinii to be a

member of the Fungi. *Nature* **334,** 519–522 (1988).

81. Henshaw, N. G., Carson, J. L. & Collier, A. M. Ultrastructural Observations of Pneumocystis carinii Attachment to Rat Lung. 181–186 (1985).

82. Young, L. S. Pneumocystis carinii Pneumonia. *Lenfant C, ed. Lung Biol.* **22,** 243 (1984).

83. Kelly, M. N. & Shellito, J. E. Current understanding of Pneumocystis immunology. *Future Microbiol.* **5,** 43–65 (2010).

84. Wang, J., Wright, T. W. & Gigliotti, F. Immune modulation as adjunctive therapy for Pneumocystis pneumonia. *Interdiscip. Perspect. Infect. Dis.* **2011,** (2011).

85. Lemiale, V., Debrumetz, A., Delannoy, A., Alberti, C. & Azoulay, E. Adjunctive steroid in HIV-negative patients with severe Pneumocystis pneumonia. *Respir. Res.* **14,** 87 (2013).

86. Cliffe, S. T. *et al.* Clinical, molecular, and cellular immunologic findings in patients with SP110-associated veno-occlusive disease with immunodeficiency syndrome. *J. Allergy Clin. Immunol.* **130,** 735–742.e6 (2012).

87. Schneider, U., Schwenk, H.-U. & Bornkamm, G. Characterization of EBV-genome negative ‘null’ and ‘T’ cell lines derived from children with acute lymphoblastic leukemia and leukemic transformed non-Hodgkin lymphoma. *Int. J. Cancer* (1977).

88. Marquardsen, F. A. *et al.* Detection of Sp110 by Flow Cytometry and Application to Screening Patients for Veno-occlusive Disease with Immunodeficiency. *J. Clin. Immunol.* **37,** 707–714 (2017).

89. Pfaffl, M. W. A new mathematical model for relative quantification in real-time RT-PCR. *Nucleic Acids Res.* **29,** 45e–45 (2001).

90. Wang, T., Ong, P., Roscioli, T., Cliffe, S. T. & Church, J. A. Hepatic veno-occlusive disease with immunodeficiency (VODI): First reported case in the U.S. and identification of a unique mutation in Sp110. *Clin. Immunol.* **145,** 102–107 (2012).

91. Bofill, M. *et al.* Laboratory control values for CD4 and CD8 T lymphocytes. Implications for HIV-1 diagnosis. *Clin. Exp. Immunol.* **88,** 243–252 (1992).

92. Gigliotti, F. & Wright, T. W. Immunopathogenesis of Pneumocystis carinii pneumonia. *Expert Rev. Mol. Med.* **7,** 1–16 (2005).

93. Downward, J., Graves, J. D., Warne, P. H., Rayter, S. & Cantrell, D. A. Stimulation of

p21ras upon T-cell activation. *Nature* **346,** 719–723 (1990).

94. Liu, B. *et al.* ABL-N-induced apoptosis in human breast cancer cells is partially mediated by c-Jun NH2-terminal kinase activation. *Breast Cancer Res.* **12,** R9 (2010).

95. Melero-Fernandez de Mera, R. M. *et al.* A simple optogenetic MAPK inhibitor design reveals resonance between transcription-regulating circuitry and temporally-encoded inputs. *Nat. Commun.* **8,** 15017 (2017).

96. Schneider, A. G., Abi Abdallah, D. S., Butcher, B. A. & Denkers, E. Y. Toxoplasma gondii triggers phosphorylation and nuclear translocation of dendritic cell STAT1 while simultaneously blocking IFNgamma-induced STAT1 transcriptional activity. *PLoS One* **8,** e60215 (2013).

97. Kanda, M. *et al.* Leukemia Inhibitory Factor Enhances Endogenous Cardiomyocyte Regeneration after Myocardial Infarction. *PLoS One* **11,** e0156562 (2016).

98. Yue, P. *et al.* Hydroxamic Acid and Benzoic Acid-Based STAT3 Inhibitors Suppress Human Glioma and Breast Cancer Phenotypes In Vitro and In Vivo. *Cancer Res.* **76,** 652–663 (2016).

99. Ostojic, A., Vrhovac, R. & Verstovsek, S. Ruxolitinib: a new JAK1/2 inhibitor that offers promising options for treatment of myelofibrosis. *Future Oncol.* **7,** 1035–1043 (2011).

100. Scoltock, A. B. & Cidlowski, J. A. Activation of intrinsic and extrinsic pathways in apoptotic signaling during UV-C-induced death of Jurkat cells: The role of caspase inhibition. *Exp. Cell Res.* **297,** 212–223 (2004).

101. Karpel-Massler, G. *et al.* Induction of synthetic lethality in IDH1-mutated gliomas through inhibition of Bcl-xL. *Nat. Commun.* **8,** 1067 (2017).

102. Jordan, M. B., Hildeman, D., Kappler, J. & Marrack, P. An animal model of hemophagocytic lymphohistiocytosis (HLH): CD8+ T cells and interferon gamma are essential for the disorder. *Blood* **104,** 735–743 (2004).

103. Rodero, M. P. & Crow, Y. J. Type I interferon–mediated monogenic autoinflammation: The type I interferonopathies, a conceptual overview. *J. Exp. Med.* **213,** 2527–2538 (2016).

104. Sandstrom, T. S., Ranganath, N. & Angel, J. B. Impairment of the type I interferon response by HIV-1: Potential targets for HIV eradication. *Cytokine Growth Factor Rev.* **37,** 1–16 (2017).

105. Rodero, M. P. *et al.* Detection of interferon alpha protein reveals differential levels and cellular sources in disease. 1547–1555 (2017).

106. Waldmann, I., Walde, S. & Kehlenbach, R. H. Nuclear import of c-Jun is mediated by multiple transport receptors. *J. Biol. Chem.* **282,** 27685–27692 (2007).

107. Schreck, I. *et al.* c-Jun localizes to the nucleus independent of its phosphorylation by and interaction with JNK and vice versa promotes nuclear accumulation of JNK. *Biochem. Biophys. Res. Commun.* **407,** 735–740 (2011).

108. Salomoni, P. *et al.* The promyelocytic leukemia protein PML regulates c-Jun function in response to DNA damage The promyelocytic leukemia protein PML regulates c-Jun function in response to DNA damage. **105,** 3686–3690 (2012).

109. Dong, C. *et al.* Defective T Cell Differentiation in the Absence of JNK1. *Science (80-.).* **282,** 2092–2095 (1998).

110. Chhabra, A., Mukherji, B. & Batra, D. Activation induced cell death (AICD) of human melanoma antigen-specific TCR engineered CD8 T cells involves JNK, Bim and p53. *Expert Opin. Ther. Targets* **21,** 117–129 (2017).

111. Mehrotra, S., Chhabra, A., Hegde, U., Chakraborty, N. G. & Mukherji, B. Inhibition of c-Jun N-terminal kinase rescues influenza epitope-specific human cytolytic T lymphocytes from activation-induced cell death. *J. Leukoc. Biol.* **81,** 539–547 (2007).

112. Mehrotra, S. *et al.* Rescuing melanoma epitope-specific cytolytic T lymphocytes from activation-induced cell death, by SP600125, an inhibitor of JNK: implications in cancer immunotherapy. *J. Immunol.* **173,** 6017–6024 (2004).

113. Voos, P. *et al.* Ionizing Radiation Induces Morphological Changes and Immunological Modulation of Jurkat Cells. *Front. Immunol.* **9,** 922 (2018).

114. Kiessling, M. K. *et al.* Inhibition of NF-kappaB induces a switch from CD95L-dependent to CD95L-independent and JNK-mediated apoptosis in T cells. *FEBS Lett.* **584,** 4679–4688 (2010).

115. Zhang, Y., Xing, D. & Liu, L. PUMA promotes Bax translocation by both directly interacting with Bax and by competitive binding to Bcl-X L during UV-induced apoptosis. *Mol. Biol. Cell* **20,** 3077–3087 (2009).

116. Bronke, C., Westerlaken, G. H. A., Miedema, F., Tesselaar, K. & van Baarle, D. Progression to CMV end-organ disease in HIV-1-infected individuals despite

abundance of highly differentiated CMV-specific CD8+ T-cells. *Immunol. Lett.* **97,** 215–224 (2005).

117. Barry, S. M., Johnson, M. A. & Janossy, G. Cytopathology or immunopathology? The puzzle of cytomegalovirus pneumonitis revisited. *Bone Marrow Transplant.* **26,** 591–597 (2000).

118. Shah, P. D., Zhong, Q., Lendermon, E. A., Pipeling, M. R. & McDyer, J. F. Hyperexpansion of Functional Viral-Specific CD8+ T Cells in Lymphopenia-Associated MCMV Pneumonitis. *Viral Immunol.* **28,** 255–264 (2015).

119. Noel, N. *et al.* Interferon-associated therapies toward HIV control: The back and forth. *Cytokine Growth Factor Rev.* **40,** 99–112 (2018).

120. Baechler, E. C. *et al.* Interferon-inducible gene expression signature in peripheral blood cells of patients with severe lupus. *Proc. Natl. Acad. Sci. U. S. A.* **100,** 2610–2615 (2003).

121. Wouters, C. H. P., Diegenant, C., Ceuppens, J. L., Degreef, H. & Stevens, E. A. M. The circulating lymphocyte profiles in patients with discoid lupus erythematosus and systemic lupus erythematosus suggest a pathogenetic relationship. *Br. J. Dermatol.* **150,** 693–700 (2004).

122. Schoenborn, J. R. & Wilson, C. B. Regulation of interferon-gamma during innate and adaptive immune responses. *Adv. Immunol.* **96,** 41–101 (2007).

123. Flynn, J. L. *et al.* An Essential Role for Interferon 7 in Resistance to Mycobacterium tuberculosis Infection. *J. Exp. Med.* **178,** 2249–54 (1993).

124. Locatelli, F. *et al.* A Novel Targeted Approach to the Treatment of Hemophagocytic Lymphohistiocytosis (HLH) with an Anti-Interferon Gamma (IFNγ) Monoclonal Antibody (mAb), NI-0501: First Results from a Pilot Phase 2 Study in Children with Primary HLH. *Blood* **126,** LBA-3 LP-LBA-3 (2015).

125. Ishimine, T., Kawakami, K., Nakamoto, A. & Saito, A. Analysis of cellular response and gamma interferon synthesis in bronchoalveolar lavage fluid and lung homogenate of mice infected with Pneumocystis carinii. *Microbiol. Immunol.* **39,** 49–58 (1995).

126. Pesanti, E. L. Interaction of cytokines and alveolar cells with Pneumocystis carinii in vitro. *J. Infect. Dis.* **163,** 611–616 (1991).

127. Rook, G. A. Role of activated macrophages in the immunopathology of tuberculosis.

Br. Med. Bull. **44,** 611–623 (1988).

128. Schroder, K., Hertzog, P. J., Ravasi, T. & Hume, D. A. Interferon-gamma: an overview of signals, mechanisms and functions. *J. Leukoc. Biol.* **75,** 163–189 (2004).

129. Barry, M. & Bleackley, R. C. Cytotoxic T lymphocytes: all roads lead to death. *Nat. Rev. Immunol.* **2,** 401–409 (2002).